From rift to drift in South Pamir (Tajikistan): Permian evolution of a Cimmerian terrane

L. Angiolini [a], A. Zanchi [b], S. Zanchetta [b], A. Nicora [a], I. Vuolo [a], F. Berra [a], C. Henderson [c], N. Malaspina [b], R. Rettori [d], D. Vachard [e], G. Vezzoli [b]

[a] Dipartimento di Scienze della Terra ''A. Desio'', Via Mangiagalli 34, 20133 Milano, Italy [b] Dipartimento di Scienze dell'Ambiente e del Territorio e di Scienze della Terra, Piazza della Scienza 4, 20126 Milano, Italy [c] Department of Geoscience, University of Calgary, Calgary, Alberta T2N1N4, Canada [d] Dipartimento di Fisica e Geologia, Via Pascoli, 06123 Perugia, Italy

[e] Université de Lille1, UFR Sciences Terre, UMR CNRS 8217 Géosystèmes, 59655 Villeneuve d'Ascq Cédex, France

ABSTRACT

Here, we describe the Permian–Lower Triassic sedimentary succession of South Pamir and the associated biota of conodonts, foraminifers and brachiopods. The studied succession comprises the CarboniferousLower Permian siliciclastic Uruzbulak and Tashkazyk formations (Bazar Dara Group), which are unconformably covered by upper Lower to Upper Permian units, deposited both in platform settings (Kurteke Formation), and on the slope and basin (Kochusu Formation, Shindy Formation, Kubergandy Formation, Gan Formation, and Takhtabulak Formation). These formations comprise bioclastic limestones, cherty limestones, shales, volcaniclastic rocks, basalts, sandstones and conglomerates, and are locally very rich in fossils (fusulinids, ammonoids, brachiopods, corals and conodonts). The Permian succession is then overlain by shallow water carbonates of the Induan to Anisian Karatash Group. Subsidence analysis and volcanics of the Permian and overlying Triassic successions constrains the timing of rifting of South Pamir from Gondwana in the Early Permian (=Cisuralian), and its docking to Central Pamir, the Eurasian margin and the interposed volcanic arcs at the end of the Triassic. The sedimentary successions of the Pamirs represent a key-point to refine the correlations between the Tethyan regional scale and the International Time Scale. The analyses of the fusulinids and conodonts of the Kubergandian and Murgabian stratotypes of SE Pamir suggest that: (1) the upper Bolorian and the lower part of the Kubergandian correlate to the upper Kungurian; (2) the upper Kubergandian and the lower Murgabian correlate to the Roadian; (3) the mid-upper Murgabian correlates to the Wordian; (4) possibly the uppermost Murgabian and the lower Midian correlate to the lower Capitanian.

The Kubergandian is thus a defined regional stage, based on fusulinids, ammonoids and conodonts and can be correlated to the Kungurian and the Roadian; still problematic remains the Murgabian correlation which needs to be investigated and resolved in other Tethyan sections.

1. Introduction

The tectonic setting that characterizes nowadays Central Asia is the results of a complex evolution that started at the beginning of the Mesozoic with the progressive accretion of several blocks of Perigondwanan ancestry to the Eurasian margin and the closure of the Palaeotethys ocean by subduction beneath the southern Eurasia margin (Zanchetta et al., 2013 and references therein). This geodynamic event, traceable from Iran to Tibet through Central Asia, is known as Cimmerian orogeny and it is bracketed in time between the Late Triassic and the Early Jurassic (e.g. Sengör, 1979; Gaetani, 1997; Schwab et al., 2004; Zanchi et al., 2009; Zanchi and Gaetani, 2011; Robinson et al., 2012; Angiolini et al., 2013a, 2013b). However, the events leading to this complex tectonic evolution started much earlier than the Mesozoic, in the Late Carboniferous-Early Permian. This time witnessed the progressive distinction and detachment of the Cimmerian terranes – including Iran, Central Afghanistan, Karakorum, Central and South Pamir, and Sibumasu – which broke off from the Gondwanan margin and drifted northward with the opening of the Neotethys Ocean (Sengör, 1979; Gaetani, 1997; Angiolini et al., 2003, 2007; Muttoni et al., 2009; Domeier and Torsvik, 2014).

South Pamir, one of the main orogenic belts which form the Pamirs (e.g. Yin and Harrison, 2000; Schwab et al., 2004; Robinson et al., 2012; Angiolini et al., 2013a) (Fig. 1), results from the Late Triassic collision of a Cimmerian block- broken off the Gondwanan margin in the Early Permian- with Central Pamir. This in turn was colliding with the southern Eurasian margin and the interposed volcanic arcs (Karakul-Mazar belt) at the end of the Triassic (Cimmerian orogeny) (e.g. Sengör, 1979; Gaetani, 1997; Schwab et al., 2004; Zanchi et al., 2009; Muttoni et al., 2009; Zanchi and Gaetani, 2011; Robinson et al., 2012; Angiolini et al., 2013a, 2013b). The South Pamir belt was later deformed during the Mesozoic and finally during the Caenozoic by collision and indentation of India (Burtman and Molnar, 1993; Replumaz et al., 2014).

Understanding the Permian-Triassic evolution of South Pamir is thus very important to add further constraints on the differential motions of the Cimmerian terranes at the Palaeozoic-Mesozoic transition.

If considerable efforts were done so far to reconstruct the palaeobiogeographic affinity, the tectonic deformation and the timing of accretion of South Pamir to Eurasia (e.g. Dronov and Leven, 1990; Vlasov et al., 1991; Schwab et al., 2004; Robinson et al., 2012; Angiolini et al., 2013a), less information is available on its sedimentary evolution during Permian and on the tempo of its detachment from Gondwana and early northward drift. This information is recorded in the sedimentary successions spectacularly cropping out in the Gorno-Badakhshan Autonomous Region of Southeast Pamir, Tajikistan (hereafter SE Pamir) (Fig. 1).

The goal of this paper is to document in detail the stratigraphic evolution of the Upper Palaeozoic sedimentary basins of the South Pamir terrane, and, through subsidence analysis, to constrain the timing of its rifting from the Gondwana margin and the subsequent drifting during Permian.

The sedimentary succession of SE Pamir represents also a keypoint to refine the correlations between the Tethyan chronostratigraphic scale and the International Time Scale. Therefore, this paper is also aimed to contribute to the discussion on the Middle Permian (=Guadalupian) correlation, hotly debated by the Subcommission on Permian Stratigraphy of the International Commission on Stratigraphy, IUGS.

2. Geological setting

South Pamir is separated from Central Pamir by the RushanPshart zone (Pashkov and Budanov, 1990; Leven, 1995; Burtman, 2010; Robinson et al., 2012; Angiolini et al., 2013a). South Pamir is bounded southward by Karakoram, but their contact is still debated, some authors considering them to be continuous (e.g. Schwab et al., 2004; Robinson et al., 2012); others authors (Zanchi et al., 2000; ZanchiandGaetani,2011) seek for aminorsuture zone alongthe Tirich Boundary Zone (TBZ) where serpentinized mantle peridotites may represent the remnants of a secondary suture zone (Fig. 1). The southwestern part of South Pamir consists of metamorphic rocks exhumed in the Cenozoic following the Indian plate collision (Schmidtetal., 2011;Stübneretal., 2013a,2013b). Thesoutheastern region of South Pamir, i.e. SE Pamir, shows a thick Permian to

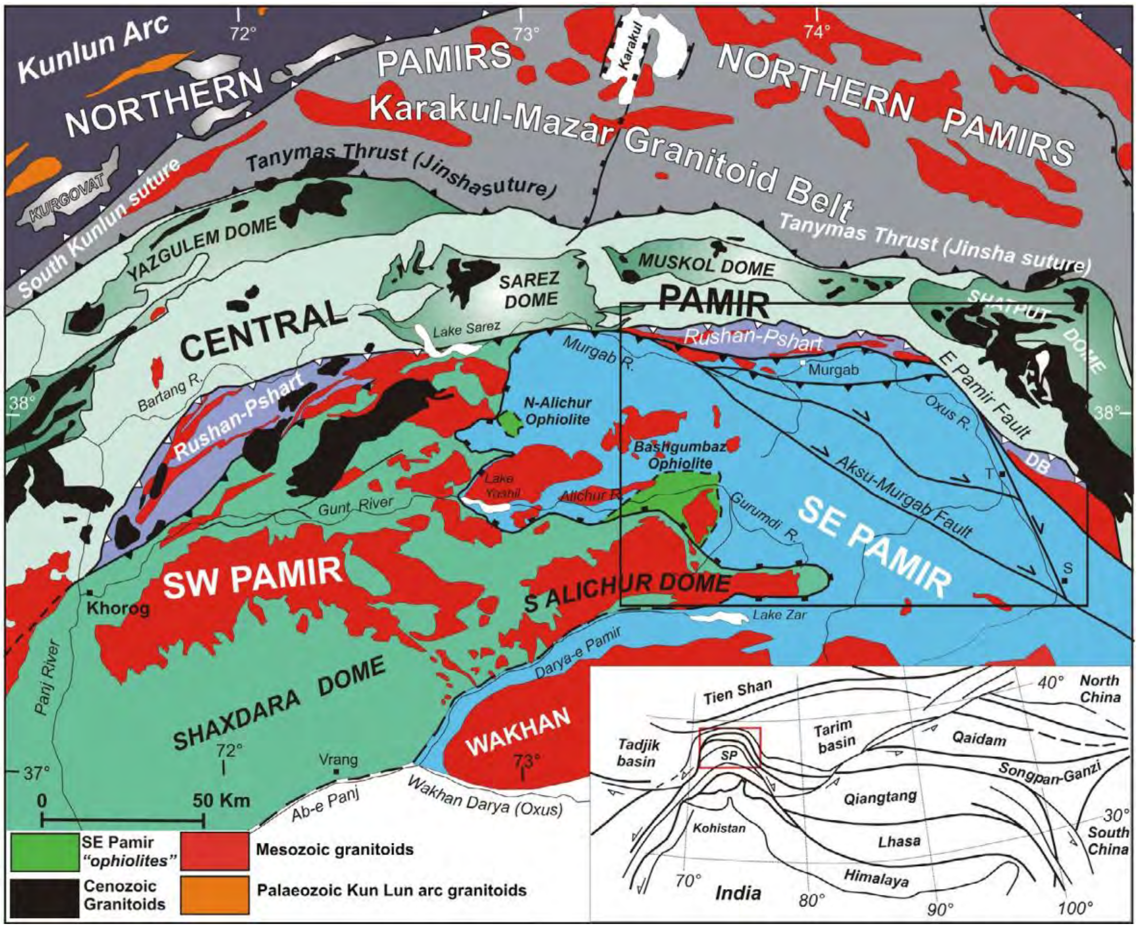

Fig. 1. Tectonic setting of SE Pamir, C Pamir and N Pamir, located between the Eurasian plate to the north and the Karakorum, Kohistan/Ladakh and the Indian plate to the south. The studied area is outlined in red. KKSZ: Karakoram–Kohistan suture zone; MMT: Main mantle thrust. Modified from Angiolini et al. (2013a) (For interpretation of the references to colour in this figure legend, the reader is referred to the web version of this article.).

Cenozoic sedimentary succession, stacked into a polyphase Mesozoic-Cenozoic fold and thrust belt, which escaped the important metamorphism affecting most of the surrounding units.

The Permian-Triassic sedimentary succession of SE Pamir was studied in the past by Russian authors (e.g. Dutkevich, 1937; Leven, 1967; Grunt and Dmitriev, 1973; Dronov and Luchnikov, 1976; Novikov, 1976, 1979; Chediya and Davydov, 1980; Leven, 1958, 1967, 1981; Chediya et al., 1986; Leonova and Dmitriev, 1989; Dagys and Dronov, 1989; Grunt and Novikov, 1994; Reimers, 1999; Korchagin, 2008, 2009). Angiolini et al. (2013a) presented an updated summary of the main features of the succession.

The Permian–Lower Triassic succession, which is described in detail in the following paragraphs, comprises at the base the Lower Permian Uruzbulak and Tashkazyk formations (Bazar Dara Group), consisting of fine to medium siliciclastic locally fossiliferous strata.
They are unconformably covered by an upper Lower to Upper Permian (=Lopingian) succession. This comprises both platform facies, recorded by the massive limestones of the Kurteke Formation, and slope to basinal facies, which are represented by the Kochusu Formation, Shindy Formation, Kubergandy Formation, Gan Formation, and Takhtabulak Formation. These formations consist of bioclastic limestones, cherty limestones, shales, volcaniclastic rocks, sandstones and conglomerates. The fossil content is locally very rich (fusulinids, ammonoids, brachiopods, corals and conodonts). The lower part of the overlying Triassic succession consists of platform carbonates of the Induan to Anisian Karatash Group.

Leven (1967) recognized the existence of different palaeogeographic domains with a distribution described as a horseshoe opening to the east (Leven, 1967, p. 12, Fig. 1), and structured at the end of the Early Permian. In this reconstruction, the platform facies of the Kurteke Formation lie at the core of the horseshoe, surrounded by deeper water facies (Kubergandy and Gan formations) (Leven, 1967, p. 12, Fig. 3). However, as already underlined by Leven (1967, p. 12), the observation of the lateral contacts between the different facies is hampered by the severe tectonic deformation affecting the region. This prevents a reliable reconstruction of the different domains, whose knowledge is based only on laterally discontinuous stratigraphic sections, a few measured where platform facies crop out (i.e. Kurteke) and most along the wider outcrops of the Kubergandy and Gan formations.

To study the Permian–Lower Triassic succession, we sampled the following stratigraphic sections and fossiliferous localities during summers 2010 and 2011 (Fig. 2):

Kubergandy section (3752^{0}04.4^{00}N–7337^{0}19.4^{00}E; 3950 m a.s.l.).
Mamasar Bulak (3753^{0}03.5^{00}N–7351^{0}58.8^{00}E).
Kutal 2 section (3805^{0}10.4^{00}N–7358^{0}22.4^{00}E; 3974 m a.s.l.).
Kurteke 1 section (3749^{0}51.2^{00}N–7402^{0}20.6^{00}E; 4317 m a.s.l.).
Kurteke 3 section (3750^{0}39.1^{00}N–7403^{0}03.2^{00}E; 4205 m a.s.l.). Karebeles Valley at Mudzubulak (3801^{0}43.8^{00}N–7405^{0}20.5^{00}E; 4650 m a.s.l.).
Kuristyk section (3748^{0}23.5^{00}N–7423^{0}21.2^{00}E; 4317 m a.s.l.). Kastenat Djilga section (3740^{0}53^{00}N–7427^{0}57.3^{00}E to 3740^{0}44^{00} N–7428^{0}19.3^{00}E; 4315 m a.s.l.).

Thrusts and strike-slip faults dissect the Permian succession so that the sampling was done in different tectonic units, as shown in Fig. 3. In particular, we measured most of the sections in the intermediate unit of Ruzhentsev and Shvol^{0}man (1981).

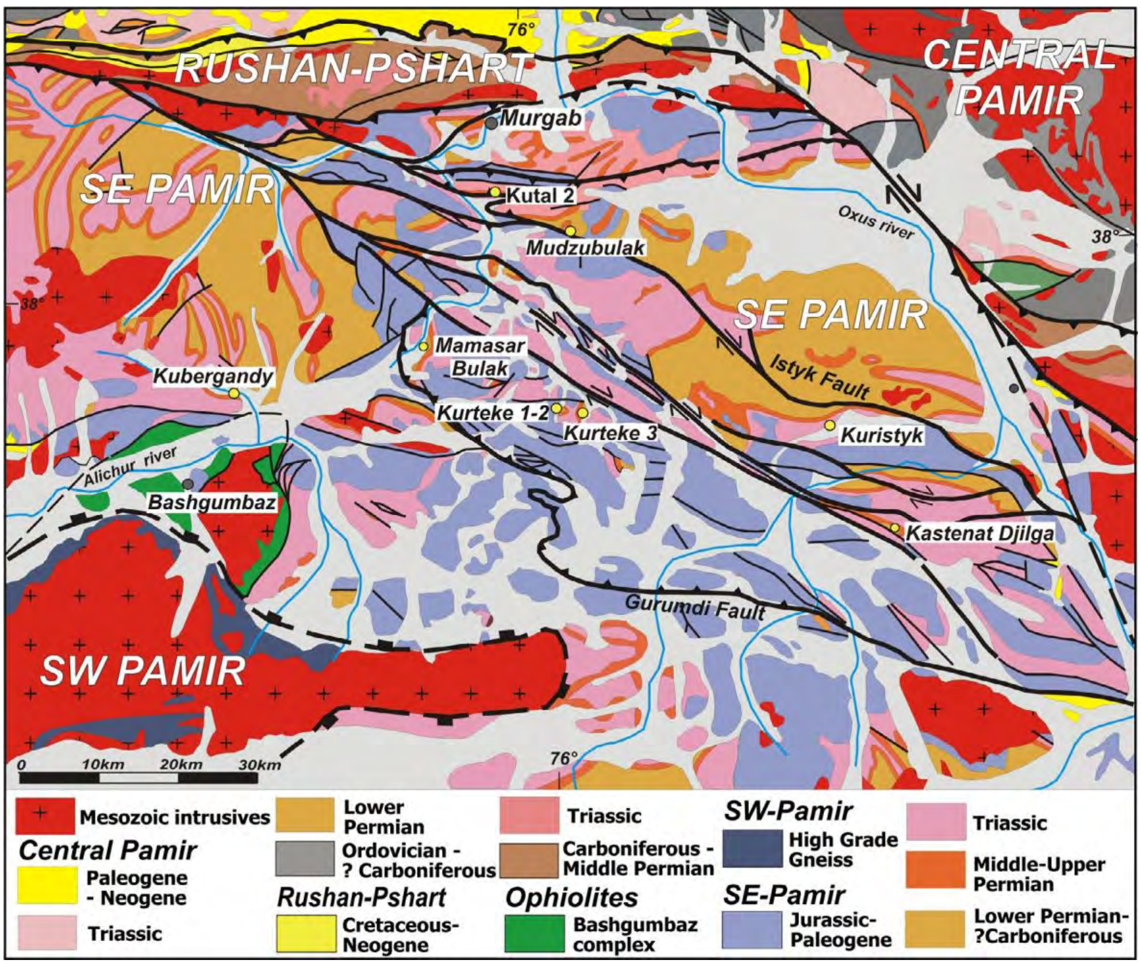

Fig. 2. Geological map of the studied area based on Angiolini et al. (2013a), showing the location of the stratigraphic logs.

Fig. 3. Stratigraphic scheme of the Permian formations with the position of the measured sections. Kt2: Kutal 2; Kub: Kubergandy; Muz: Mudzubulak; Krs: Kuristyk; Kur1: Kurteke 1; Kur3: Kurteke 3; Kas: Kastenat Djilga; Mam: Mamasar Bulak.

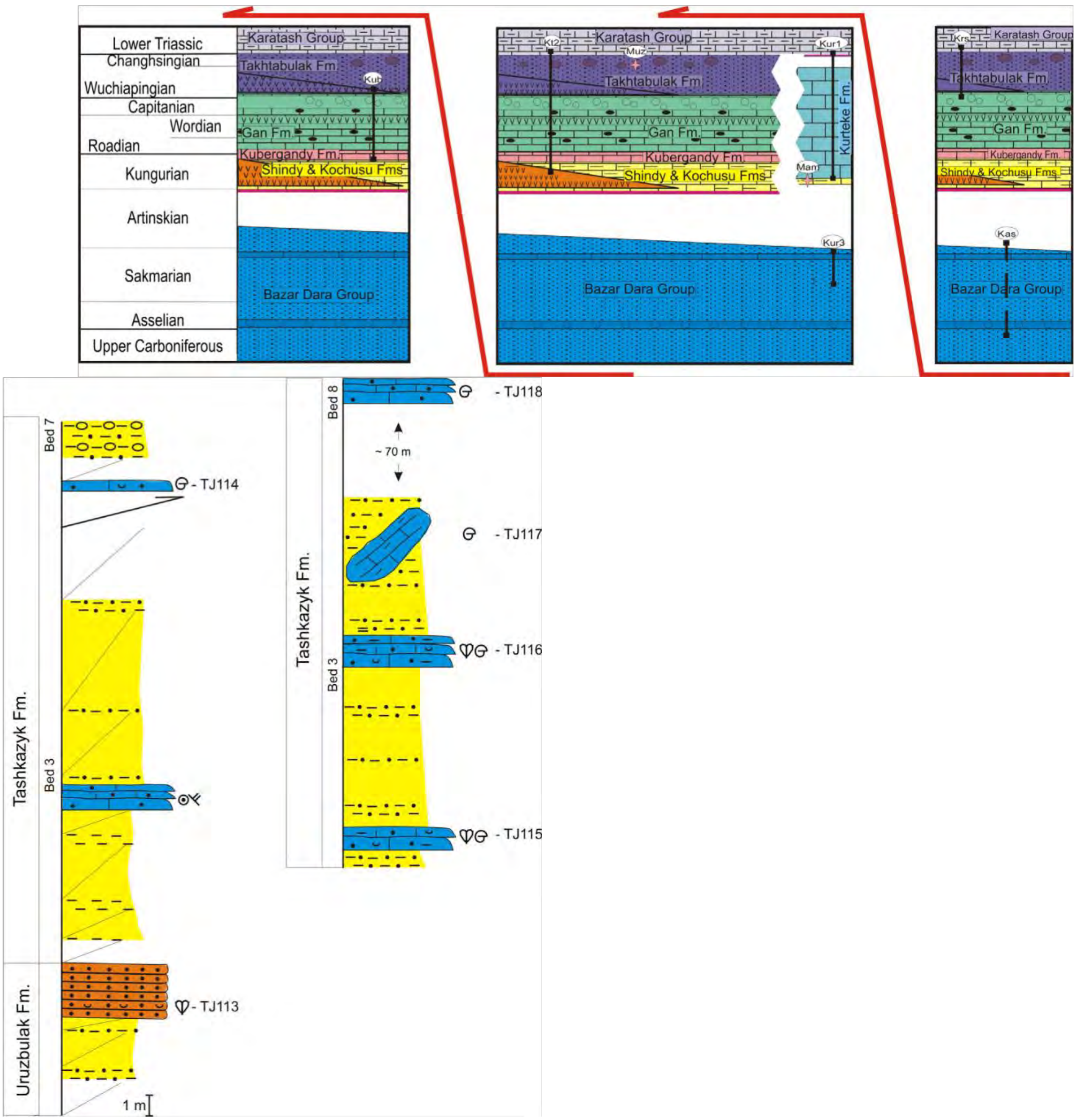

Fig. 4. Section of the Tashkazyk Formation in the Kastenat Djilga Valley. Left log starting at 3740^{0}53^{00}N–7427^{0}57.3^{00}E; right log starting at 3740^{0}44^{00}N– 7428^{0}19.3^{00}E; 4315 m a.s.l. The section has not been measured in detail as the formation was mostly covered. Legend as Fig. 5.

3. Bazardara Group (Uruzbulak and Tashkazyk formations)

Carboniferous and pre-Kungurian (uppermost Lower Permian) sedimentary rocks of SE Pamir belong to the Bazardara Group which consists of cold water siliciclastic deposits (Dutkevich, 1937). It was divided into two formations: the Uruzbulak Formation below and the Tashkazyk Formation above (Novikov, 1976). According to Grunt and Novikov (1994), the group is up to 2000 m-thick, with the Tashkazyk Formation having a total thickness of 300–980 m. However, its thickness is very variable, being greater (700–980 m) in Karabeles and North Alichur, but reduced to 300–500 m in Kastenat Djilga and Kurteke areas, where also the Uruzbulak Formation has a thickness of about 120 m (Grunt and Novikov, 1994). The lower contact of the group is not exposed.

We studied a few outcrops of the Tashkazyk Formation in the Karebeles and Kuristyk Valleys and we measured two stratigraphic sections of the formation at Kastenat Djilga and Kurteke 3 (Figs. 2– 5). In general, the outcrops of the Bazardara Group are poorly exposed and covered by talus or a thick soil cover, so that it is rather difficult to measure in detail stratigraphic sections and thicknesses (Fig. 6A).

The contact with the overlying formations is never clearly exposed both at Kurteke and at Kastenat Djilga, where it is probably faulted.

3.1. Lithology

The Uruzbulak Formation comprises black claystones and siltstones capped by bioclastic immature sandstones, bioclastic sandy limestones and siltstones. The Tashkazyk Formation consists of sandstones, siltstones and black shales with fossiliferous calcareous sandstones at the top. Sandstones from the Tashkazyk Formation are characterized by quartz (mean 79 ± 9) with K-feldspars and plagioclase (Table 1). Plutonic grains are common (Fig. 7).

The Tashkazyk Formation in the Kastenat Djilga area comprises several units, which from the base, consist of: 40–60 m of claystones, bioclastic sandy limestones, calcareous sandstones with boulders of bioclastic sandy limestones (bed 3 of Grunt and Novikov, 1994); 10 m of black claystones, siltstones and bioturbated sandstones (bed 4 of Grunt and Novikov, 1994); 25–30 m of black claystones containing yellow marlstones and lenses of limestones (bed 5 of Grunt and Novikov, 1994); 40–50 m of claystones and siltstones with concretions of calcareous siltstones (bed 6 of Grunt and Novikov, 1994); 80–125 m of silty claystones and calcareous siltstones with rare bioturbated marly limestones and with carbonate, siliceous or clayey concretions (bed 7 of Grunt and Novikov, 1994); 5–10 m of bioclastic calcareous sandstones (bed 8 of Grunt and Novikov, 1994); 20 m of black claystones and sandy siltstones with ferruginous crusts at the top suggesting emersion (bed 9 of Grunt and Novikov, 1994).

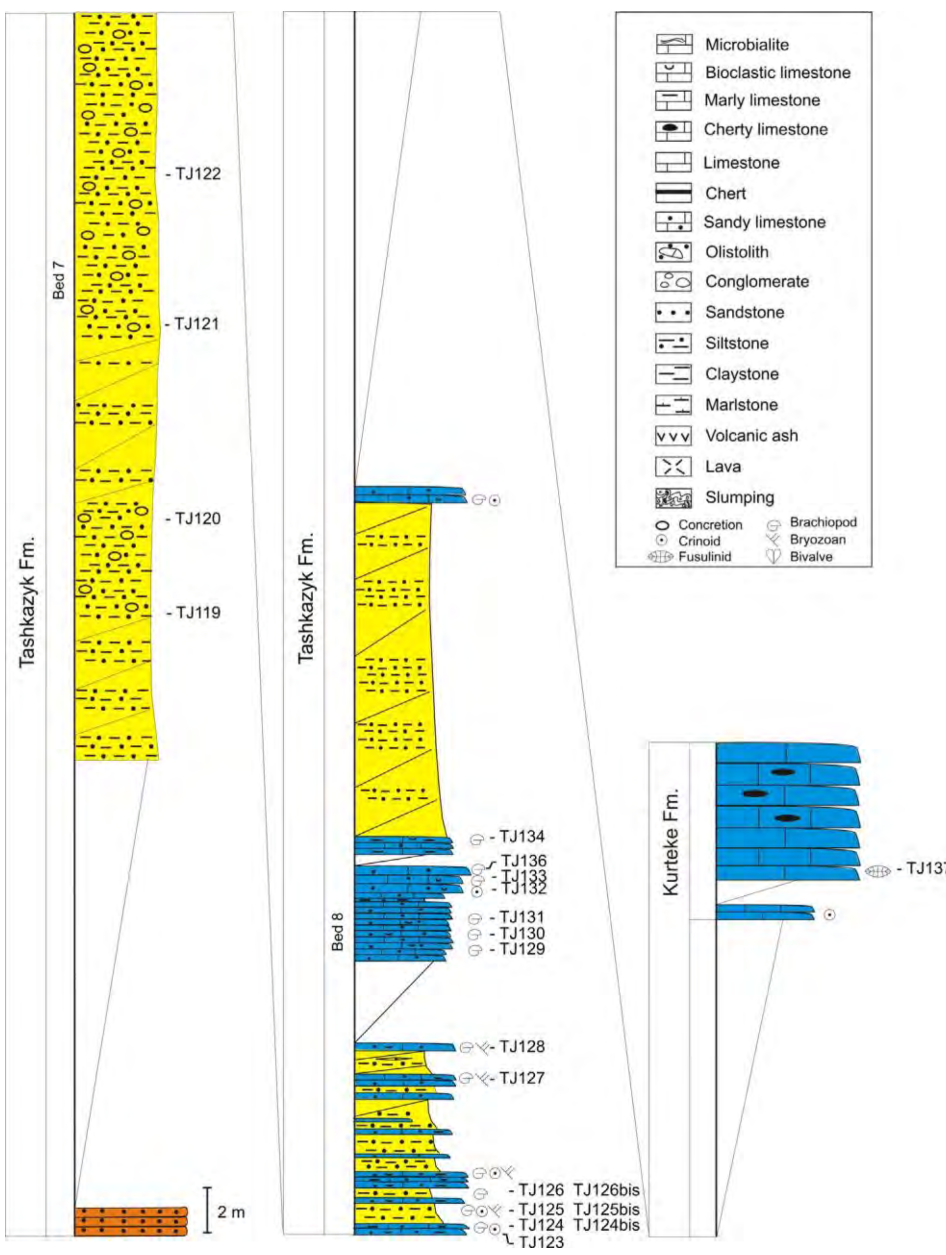

Fig. 5. Section of the upper part of the Tashkazyk Formation at Kurteke 3 locality, base of the section at $3750^{0}39.1^{00}$N–$7403^{0}03.2^{00}$E.

The ''lump-boulder'' lithozone (bed 3) at the base of the formation at Kastenat Djilga is quite distinctive with the occurrence of blocks of stratified bioclastic sandy limestones discordant to the general bedding (TJ117). Along the Kurteke 3 section only the upper part of the formation (bed 7 to 9) crops out (TJ123-136 in Fig. 6A). 3.2. Fossil content

The Uruzbulak Formation contains cold-water bivalves, conulariids, bryozoans and rare ammonoids of Carboniferous age (Leven,1967; Pavlov,1972).At thetopoftheformation,we collected a very well preserved assemblage of the infaunal bivalve Oriocrassatella sp. consisting of articulated shells mostly in life position.

The Tashkazyk Formation comprises conulariids, crinoids, bryozoans, ammonoids (Metapronorites sp., Marathonites sp., Emilites sp.), bivalves (Pseudomyalina sp., Megadesmus sp.) (Leven, 1967; Pavlov, 1972) and very abundant brachiopods. According to Grunt and Dmitriev (1973) and to our own analysis, brachiopods from the Tashkazyk Formation comprise species of Costatumulus, Permochonetes, Reticulatia, Spirelytha, Tomiopsis, and Trigonotreta.

We have found conodonts inasample collected about 100 m below the top of the Tashkazyk Formation at Mudzubulak. They comprise Mesogondolella monstra, Streptognathodus sp., Sweetognathus bucaramangus, S. cf. merrilli, S. cf. behnkeni, and S. whitei (Table 2c; Supplementary Fig. S1). Although S. whitei has normally been associated with an Artinskian age, it was determined that the holotype of S. whitei is older(Lucas,2014;Henderson, 2014).Sucholder forms from Nevada (Ritter, 1987) and Bolivia (Suarez Riglos et al., 1987) are now ascribed tothelateAsselianandearlySakmarian.AccordingtoChernykh(2005) Mesogondolella monstra is typical of the Tastubian or early Sakmarian substage and the S. merrilli Zone.

3.3. Age

According to Grunt and Novikov (1994), the Bazardara Group is Carboniferous-Early Permian in age. The rare ammonoids of the Tashkazyk Formation suggest a Late Carboniferous (=Pennsylvanian)-Early Permian age for its lower part, but the bivalves in the upper beds of the Uruzbulak Formation and in bed 3 of the Tashkazyk Formation are restricted to the Sakmarian-Artinskian (Grunt and Novikov, 1994).

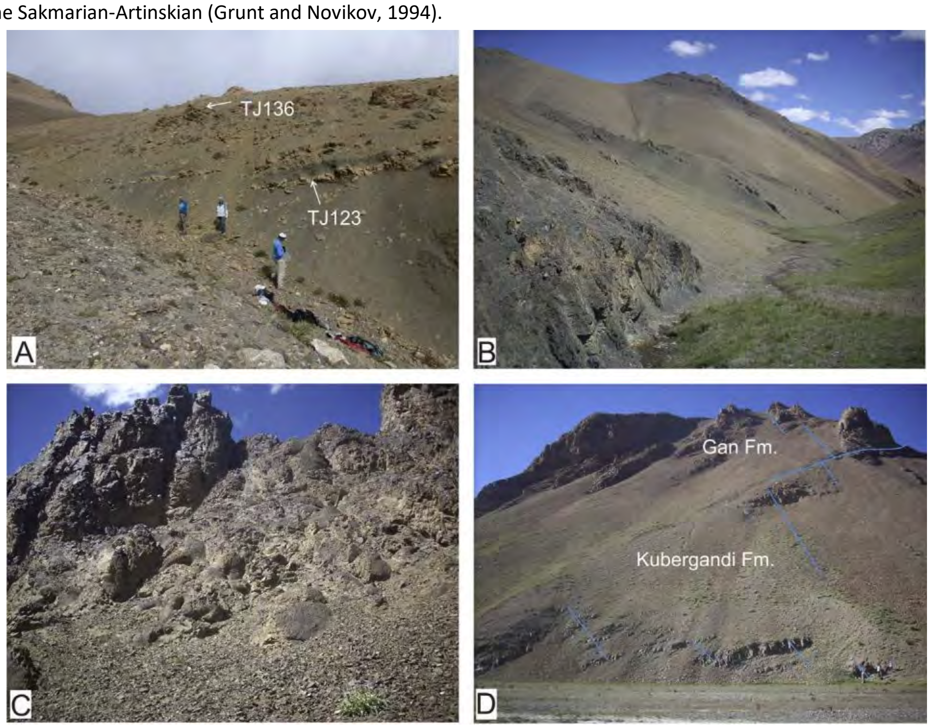

Fig. 6. (A) Fossiliferous beds TJ123 to TJ136, Kurteke 3 section. (B) Tashkazyk and Kochusu formations in the Kuristyk Valley. The Kochusu is the whitish interval in the right. The prominent beds in the foreground are the sandstones of the Tashkazyk Formation. (C) Shindy Formation in the Kuristyk Valley. Massive basaltic lava flows with pillow texture (sample TZ18-19). (D) Photo of the Kubergandy type-section. Base: 3752^{0}04.4^{00}N–7337^{0}19.4^{00}E; 3950 m a.s.l.

Table 1

Detrital modes of sandstones of the Bazardara and Taktabulak formations. Q = quartz; KF = K-feldspar; P = plagioclase; Lvf = felsic volcanic lithic fragments; Lvm = mafic volcanic lithic fragments; Lcc = calcareous lithic fragments; Lcd = dolomitic lithic fragments; Ls = pelitic terrigenous lithic fragments; Lch = chert lithic fragments; Lm = metamorphic lithic fragments. Percent micas (Ms, Bt) calculated on total framework grains.

	Sample	Q	KF	P	Lvf	Lvm	Lcc	Lcd	Ls	Lch	Lm	Ms	Bt	Total
Bazardara Fm.	TJ77	68.3	16.0	15.3	0.0	0.0	0.0	0.0	0.0	0.0	0.0	0.3	0.0	100.0
Carboniferous	TJ78	86.5	2.0	4.5	1.0	0.0	0.0	0.0	0.0	0.0	0.0	6.0	0.0	100.0
Lower Permian	TJ83	82.3	1.3	7.4	1.3	0.0	4.8	0.0	0.0	0.0	0.4	2.6	0.0	100.0
Taktabulak Fm.	TJ69	2.1	0.0	2.5	2.5	93.0	0.0	0.0	0.0	0.0	0.0	0.0	0.0	100.0
Upper Permian	TJ70	1.1	0.0	1.1	0.5	96.1	1.1	0.0	0.0	0.0	0.0	0.0	0.0	100.0
	TJ71	0.8	0.0	0.0	0.0	99.2	0.0	0.0	0.0	0.0	0.0	0.0	0.0	100.0
	TJ72	0.0	0.0	0.0	0.5	99.5	0.0	0.0	0.0	0.0	0.0	0.0	0.0	100.0
	TJ73	0.0	0.0	0.8	1.5	97.7	0.0	0.0	0.0	0.0	0.0	0.0	0.0	100.0

TJ74	4.0	0.0	3.4	2.0	90.6	0.0	0.0	0.0	0.0	0.0	0.0	0.0	100.0

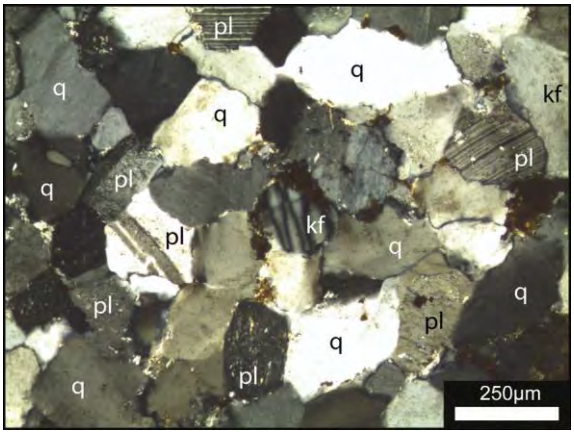

Fig. 7. Quartzose sandstone (q = quartz) with feldspars (pl = plagioclase, kf = K-feldspar).

The upper part of the Tashkazyk Formation was said to contain an assemblage of upper Asselian ammonoids (Ruzhentsev, 1978); however, its stratigraphic position is not strictly constrained. Upper Sakmarian to possibly lower Artinskian brachiopods and bryozoans occur in the upper part of Tashkazyk Formation (Grunt and Dmitriev, 1973; Gorjunova, 1975; Grunt and Novikov, 1994). Our brachiopod data indicate a Sakmarian age for the upper part of the formation and the findings of conodonts in the Tashkazyk Formation in the Mudzubulak valley suggests an age very close to the Asselian-Sakmarian boundary at about 100 m from the top of the formation, due to the co-occurrences of Sweetognathus cf. behnkeni, S. bucaramangus, S. cf. merrilli, and S. whitei (Chuvashov et al., 2013).

Table 2a

Range chart of conodonts, foraminifers (and associated microfacies) and brachiopods from Kubergandy section.

Sample	Formation	Conodonts	Foraminifers and algae	Brachiopods	Age (conodonts)	Age (foraminifers)
TJ1	Kubergandy	Mesogondolella siciliensis, Mesogondolella idahoensis (sensu latu)			Kungurian	
TJ3	Kubergandy		Tubiphytes sp., Schubertellella? sp., Parafusulina?			Bolorian
TJ4	Kubergandy		Climacammina sp.			
TJ5	Kubergandy	Mesogondolella aff. idahoensis	Eotuberitina reitlingerae, Endothyra cf. miassica, Climacammina sp. Globivalvulina ex gr. bulloides, Schubertella sp., Cornuspira sp., Nodosinelloides sp., Pachyphloia sp			Bolorian
TJ6	Kubergandy	Mesogondolella siciliensis, Mesogondolella idahoensis	Climacammina sp. Globivalvulina ex gr. bulloides, Schubertella sp.			
TJ7	Kubergandy	Pseudohindeodus ramovsi, Hindeodus cf. excavatus, Pseudohindeodus sp. A, Mesogondolella siciliensis, Sweetognathus subsymmetricus			Kungurian	
TJ8	Kubergandy	Mesogondolella sp.	Climacammina sp. Retroseptellina? sp. Neofusulinella cf. giraudi, Parafusulina? cf. dzamantalensis			Kubergandian
TJ9	Kubergandy	Hindeodus cf. excavatus, Mesogondolella siciliensis, Mesogondolella lamberti (possibly transitional forms to M. pingxiangensis)	Eotuberitina sp.		Kungurian	
TJ11	Kubergandy	Ramiforms, Hindeodus excavatus, Mesogondolella siciliensis	Schubertella sp.			
TJ12	Kubergandy	Mesogondolella pingxiangensis, Mesogondolella siciliensis, Sweetognathus cf. bicarinum	Epimastopora sp., Eotuberitina sp., Tetrataxis sp., Deckerella sp., Climacammina sp., Sphaerulina sp., Neofusulinella sp., Cancellina sp., Parafusulina sp., Pseudovermiporella sp., Pachyphloia sp.		Early Roadian	Kubergandian
TJ13	Kubergandy		Tubiphytes sp., Eotuberitina sp., Endothyra sp., Tetrataxis sp., Globivalvulina sp., Neofusulinella cf. giraudi, Geinitzina sp., Pachyphloia ovata			
TJ14	Kubergandy		Archaeolithoporella hidensis, Tubiphytes obscurus, Eotuberitina reitlingerae, Deckerella sp., Climacammina sp., Globivalvulina cf. vonderschmitti, Neofusulinella sp., Parafusulina sp., Cancellina cf. primigena, Geinitzina sp., Pachyphloia sp.			Kubergandian
TJ15	Kubergandy	Fragments	Archaeolithoporella hidensis, Tubiphytes obscurus, Gyroporella? sp., Velebitelleae n. gen., Efluegelia johnsoni, Stacheoides n. sp., Eotuberitina reitlingerae, Lasiodiscus tenuis, Endothyra sp., Neoendothyra reicheli, Tetratraxis sp., Polytaxis sp., Climacammina sp., Dagmarita sp., Schuberella sp., Neofusulinella sp., Parafusulina sp., Cancellina primigena, Hedraites sp., Ataxophragmiidae? gen. sp., Geinitzina sp., Pseudolangella sp., Pachyphloia cf. schwageri			Kubergandian
TJ16	Kubergandy	Fragments	Tubiphytes obscurus, Eotuberitina sp., Climacammina sp., Parafusulina sp.			
TJ17	Kubergandy	Ramiforms, Mesogondolella sp.	Tubiphytes obscurus, Tetrataxis sp., Climacammina sp., Schubertella sp., Cancellina sp., Midiella sp.			Kubergandian
TJ18	Gan					
TJ19	Gan	Mesogondolella sp.	Eotuberitina sp.			
TJ20	Gan	Mesogondolella sp.	Eotuberitina sp.		Roadian	
TJ21	Gan	Mesogondolella siciliensis, fragments			Roadian	

TJ22	Gan	Transition between Sweeetognathus guizhouensis and S. subsymmetricus, Mesogondolella siciliensis, Mesogondolella pingxiangensis			Roadian	
TJ23	Gan		Tubiphytes obscurus, Globivalvulina sp., Schubertella sp., Parafusulina sp., Pseudovermiporella nipponica, Graecodiscus? sp.			
TJ24	Gan	Fragments, Mesogondolella siciliensis			Roadian	
TJ25	Gan	Mesogondolella cf. siciliensis				
TJ26	Gan	Transition between Sweetognatus subsymmetricus and S. iranicus hanzongensis, Mesogondolella siciliensis, Mesogondolella omanensis			Wordian	
TJ27	Gan	Mesogondolella cf. siciliensis				
TJ29	Gan	Sweeetognathus fengshanensis, Clarkina xuanhanensis, Mesogondolella omanensis			Capitanian	
TJ30	Gan	Hindeodus wordensis, Mesogondolella omanensis				
TJ31	Gan	Mesogondolella cf. aserrata, Mesogondolella omanensis			Wordian?	
TJ32	Gan	Mesogondolella sp.	Geinitzina sp.			
TJ34	Gan	Hindeodus wordensis, Mesogondolella altudaensis			Capitanian	

Table 2b

Range chart of conodonts, foraminifers (and associated microfacies) and brachiopods from Kutal II section.

Sample	Formation	Conodonts	Foraminifers and algae	Brachiopods	Age (conodonts)	Age (foraminifers)
TJ35	Shindy		Endothyra? sp., Schubertella sp., Midiella sp.			
TJ36	Kubergandy		Endothyra sp., Schubertella sp., Calcitornella sp., Midiella sp., Geinitzina sp.			
TJ37	Kubergandy		Tubiphytes obscurus, Misellina aliciae, Parafusulina sp., Calcitornella sp., Midiella sp.			Bolorian
TJ38	Kubergandy	Mesogondolella sp.	Epimastopora japonica, Tubiphytes obscurus, Polytaxis sp., Climacammina sp., Schubertella sp., Misellina termieri, Misellina sp.			Bolorian
TJ39	Kubergandy		Codiaceae indet., Epimastopora cf. japonica, Tubiphytes obscurus, Tetrataxis sp., Climacammina sp., Schubertella? sp. (or Neofusulinella? or Yangchienia?), Nodosinellodes cf. mirabilis, Pachyphloia schwageri			
TJ40	Kubergandy		Eotuberitina sp., Tubiphytes obscurus, Climacammina sp., Globivalvulina bulloides, Schubertella sp. Neofusulinella sp. Parafusulina? sp., Pseudovermiporella nipponica, Pachyphloia cuekuerkoeyi			
TJ41	Kubergandy		Tubiphytes obscurus, Deckerella sp., Climacammina sp., Globivalvulina sp., Schubertella or Neofusulinella? sp., Parafusulina sp., Midiella sp.			Kubergandian
TJ42	Kubergandy	Mesogondolella lamberti; Mesogondolella siciliensis	Tubiphytes obscurus, Eotuberitina sp., Lasiodiscus tenuis, Endothyra sp., Neoendothyranella?, sp., Bradyina? sp., Climacammina sp., Deckerella sp., Globivalvulina bulloides, Schubertella sp., Neofusulinella sp., Hemigordiellina sp., Geinitzina sp.			
TJ43	Kubergandy		Hemigordius sp.			
TJ44	Kubergandy		Hemigordiellina regularis			

TJ45	Kubergandy		Tubiphytes obscurus, Eotuberitina sp., Lasiotrochus cf. tatoiensis, Climacammina sp., Schubertella sp., Neofusulinella sp., Midiella sp., Pachyphloia ovata		
TJ46	Kubergandy		Tubiphytes obscurus, Permocalculus sp., Eotuberitina sp., Neoendothyra cf. staffelloides, Tetrataxis sp., Climacammina sp., Globivalvulina bulloides, Neofusulinella giraudi, Yangchienia cf. compressa, Parafusulina? sp., Pseudovermiporella sp., Hemigordiellina sp., Langella sp.		Kubergandian
TJ47	Kubergandy	Mesogondolella siciliensis, Mesogondolella lamberti	Tubiphytes ex gr. obscurus, Diplosphaerina sp., Lasiodiscus tenuis, Climacammina sp., Globivalvulina ex gr. bulloides, Schubertella ex gr. paramelonica, Pachyphloia ovata		
TJ48	Kubergandy		Permocalculus sp., Tubiphytes sp., Nankinella sp., Parafusulina? sp., Hemigordiellina sp.		
TJ49	Kubergandy	Mesogondolella lamberti	Tubiphytes obscurus, Postbradyina? sp., Climacammina sp., Nankinella sp., Neofusulinella giraudi, Parafusulina? sp., Pseudovermiporella nipponica		
TJ50	Kubergandy	Transitional forms Sweetognahtus guizhouensis-Sw subsymmetricus-fragments (Mesogondolella siciliensis?)	Eotuberitina sp.		
TJ51	Gan	Transitional forms Sweetognathus guizhouensis-Sw. subsymmetriscus, Mesogondolella lamberti; Mesogondolella siciliensis	Tubiphytes ex gr. obscurus, Eotuberitina reitlingerae, Endothyra sp., Postendothyra sp., Polytaxis sp., Climacammina sp., Globivalvulina sp., Schubertetella ex gr. melonica, Pseudodoliolina? sp., Hemigordiellina sp. Geinitzina aff. spandeli, Pachyphloia ovata	Kungurian	
TJ52	Gan	Mesogondolella lamberti; Mesogondolella pingxiangensis; Sweetognathus subsymmetricus		Roadian	
TJ53	Gan	Mesogondolella pingxiangensis			
TJ55	Gan	Jinogondolella nankingensis?			
TJ56	Gan	Fragments			
TJ58	Gan	Mesogondolella siciliensis; Mesogondolella omanensis		Wordian	
TJ59	Gan	Mesogondolella siciliensis			
TJ60	Gan	Transitional forms Sweetognathus guizhouensis-Sw. subsymmetriscus; Mesogondolella siciliensis			
TJ62	Gan	Hindeodus sp.; Jinogondolella aserrata ?			
TJ63	Gan	Pseudohindeodus ramovsi; Hindeodus wordensis; Mesgondolella omanensis; Mesogondolella cf. postserrata		Capitanian	
TJ64	Gan	Mesogondolella omanensis; Mesogondolella altudaensis; Jinogondolella cf. postserrata		Capitanian	
TJ65	Gan	Mesogondolella sp.			
TJ66	Gan	Mesogondolella altudaensis	Geinitzina sp., Tubiphytes sp.		
TJ67	Gan	Iranognathus moschovitschi; Sweetognathus punctatus	Permocalculus sp., Tubiphytes sp., Globivalvulina sp., Bidagmarita sp., Reichelina pulchra, Codonofusiella sp., Pseudovermiporella longipora, Midiella sp., Multidiscus? sp., Rectostipulina quadrata, Neogeinitzina sp., Pachyphloia ovata		Wuchiapingian

Table 2c

Range chart of conodonts, foraminifers (and associated microfacies) and brachiopods from sections Kurystik (TJ84–90, 101–102), Kurteke (TJ92-97) and Mudzubulak (TJ81-82).

Sample	Formation	Conodonts	Foraminifers and algae	Brachiopods	Age (conodonts)	Age (foraminifers)

TJ81	Takhtabulak		Calcisponges			
TJ82	Tashkazyk	Streptognathodus sp., Sweetognathus bucaramangus, Sweetognathus cf. merrilli, Sweetognathus cf. behnkeni, Sweetognathus whitei, and Mesogondolella monstra			Sakmarian	
TJ84	Takhtabulak		Calcisponges and Reichelina pulchra	Costisteges sp., Enteletes dzaghrensis, Enteletes meridionalis, Martinia bisinuata, Stenoscisma armenica, Martinia aff. Warthi, Martinia rupicola, Martinia sp. 1, Martinia sp. 2, Notothyrina pontica, Notothyris pseudodjoulfensis, Heterelasmina lepton		Wuchiapingian
TJ85	Takhtabulak			Streptorhyncus aff. pelargonatus, Ortothichia avushensis, Anchorynchia sarcinifromis, Martinia aff. warthi		Wuchiapingian
TJ86	Gan		Permocalculus cf. gracilis, Deckerella sp., Tetrataxis sp., Globivalvulina sp., Dagmarita chanakchiensis, Nankinella sp., Midiella sp., Pachyphloia ovata			
TJ87	Takhtabulak		Eotuberitina sp., Tubiphytes sp., Globivalvulina? sp., Kamurana? sp.			Wuchiapingian
TJ88	Karatash	Merrillina? sp. A			Late Griesbachian	
TJ90	Karatash	Ramiforms	‘’Spirorbis‘’ phlyctaena and Claraia sp.			Induan
TJ92	Kurteke	Sweetognathus subsymmetricus, Mesogondolella lamberti, Mesogondolella siciliensis	Permcalculus? sp., Mizzia? sp., Tubiphytes obscurus, Donezella hirtipes, Eotuberitina sp., Lasiodiscus tenuis, Neondothyra cf. staffelloides, Postendothyra sp., Climacammina sp., Polytaxis? sp., Globivalvulina sp., Schubertella sp., Parafusulina? sp.		Kungurian	Lastest Kubergandian
TJ93	Kurteke	Mesogondolella siciliensis	Mizzia sp., Tubiphytes obscurus, Eotuberitina reitlingerae, Spireitlina sp., Climacammina sp., Tetrataxis sp., Globivalvulina sp., Schubertella sp., Parafusulina? cf. shakgamensis, Cancellina cutalensis, Pseudovermiporella sp., Graecodiscus n. sp., Geinitzina sp.			Latest Kubergandian
TJ94	Kurteke	Mesogondolella lamberti	Tubiphytes obscurus, Eotuberitina reitlingerae, Climacammina sp., Tetrataxis sp., Schubertella sp., Yangchienia sp., Parafusulina? cf. shakgamensis, Neoschwagerina simplex		Kungurian/ Roadian	Early Murgabian
TJ95	Kurteke	Mesogondolella sp., Mesogondolella lamberti	Climacammina sp., Tetrataxis sp., Yangchienia sp., Parafusulina? cf. annae, Neoschwagerina simplex, Praesumatrina neoschwagerinoides			eArly Murgabian
TJ97	Kurteke		Climacammina sp., gastropods, Codonofusiella sp., Pseudovermiporella sp., Globivalvulina? sp., Calcitornella sp., Nankinella sp.			Wuchiapingian
TJ101-102	Takhtabulak			Enteletella nikschitshi, Ortothichia avushensis, Notothyrina pontica		Wuchiapingian

3.4. Palaeoenvironment

The abundance of quartz and feldspars grains associated to plutonic rock fragments in the Tashkazyk sandstones are all indicative of a granitoid source.

The Tashkazyk Formation was considered a flysch by Novikov (1976, 1979) and Grunt and Novikov (1994). However, we could not find any sedimentary structure to suggest a flyschoid origin for these deposits. On the contrary, the formation shows a remarkable similarity to the Gircha Formation of Karakorum, Pakistan (Gaetani et al., 1995), which was deposited in neritic environments from nearshore to prodelta, storm dominated settings. Quantitative petrography of the two formations indicates that TJ77 is correlatable to the lower-middle Gircha Formation (Ashtigar section), whereas TJ83 is very close to the upper Gircha Formation (Ashtigar-Khudabad-Gircha).

The taxonomic composition and diversity of the brachiopods are consistent with a cold water setting, particularly the assemblages from bed 3. The limestone boulders resedimented in bed 3 are the result of tectonic activity connected to the beginning of the detachment of the Cimmerian continents.

4. Shindy and Kochusu formations

The Kochusu Formation (Dmitriev, 1976) unconformably covers the Tashkazyk Formation above an emersion surface. The Shindy Formation conformably overlays the Kochusu Formation and laterally replaces it (Leven, 1958, 1967).

Outcrops of the Kochusu Formation in the Kuristyk and Kastenat Djilga Valleys are few and mostly covered. We were not able to observe the laterite at its base, reported by Grunt and Dmitriev (1973) and Leonova and Dmitriev (1989), because it is usually covered by talus or the contact with the formation below is tectonized. Good outcrops of the Shindy Formation are present in the Kuristyk Valley, at Mudzubulak (Fig. 6B and C) and at the base of the Kutal 2 section.

4.1. Lithology

The Kochusu Formation consists of 12–60 m of silty limestones, locally bioclastic, overlain by siltstones with few and thin intercalations of marly limestones.

The Shindy Formation consists of massive basaltic lava flows with pillow texture, locally interbedded with breccias and volcaniclastic layers. The space between the pillows is filled with bioclastic limestones.

Microfacies analysis of the limestones at the base of the Kutal 2 section shows that they are bioclastic packstones with foraminifers, algae, brachiopods and bivalves.

4.2. Major and trace element compositions of the Shindy basalts

Geochemical analyses were done on the Permian basalts of the Shindy Formation from Mudzubulak (samples TZ8 and TZ9) and Kuristyk (samples TZ16, TZ17, and TZ19) and are reported in Table 3.

TZ8 and TZ9 are basaltic lava flows with porphyry texture, large altered plagioclase (and few clinopyroxene) phenocrystals and intersertal groundmass of fine-grained plagioclase and olivine, oxides and rare clinopyroxene. TZ16, TZ17, and TZ19 are olivine-rich basaltic lava flows with few phenocrystals of plagioclase and clinopyroxene.

Overall, all the analyzed samples display mafic compositions, with MgO < 10 wt.% (Fig. 8), Mg# (=Mg/(Mg + Fe^{2+})) ranging from 50 to 54 for the Mudzubulak basalts, and from 56 to 63 for the

Table 3

Bulk-rock major (wt.%) and trace (ppm) element compositions of Shindy basalts.

Sample	TZ-8	TZ-9	TZ-16	TZ-17	TZ-19
SiO_2	44.91	50.04	43.02	46.44	46.88
TiO_2	1.41	1.41	1.14	1.46	1.13
Al_2O_3	16.10	14.58	14.05	15.43	15.68
Cr_2O_3	0.03	0.03	0.09	0.02	0.02
Fe_2O_3*	9.53	10.51	8.91	11.80	10.08
MgO	4.84	6.24	7.56	7.70	8.58
MnO	0.17	0.24	0.16	0.18	0.23
P_2O_5	0.20	0.25	0.23	0.32	0.29
CaO	12.47	6.11	13.59	7.96	7.81
Na_2O	1.89	4.50	2.07	3.73	2.33
K_2O	1.80	1.42	0.81	0.52	2.46
LOI	6.30	4.30	8.00	4.10	3.80
Total	99.65	99.63	99.63	99.66	99.29
Mg#	50	54	63	56	63
Ni	40.4	46.8	244.6	48.9	49.4
Sc	38	37	38	39	42
Ba	454	574	542	233	2454
Co	37.1	35.3	50.4	35.3	40
Cs	1.7	2.7	6.3	6.5	11.7
Ga	19.4	17.5	14	17.4	15.4

Hf	2.8	4.7	2.8	2.7	2.8
Nb	13.8	25	17.3	23.9	18
Rb	39.1	25.8	27	14.9	56.1
Sr	292.3	509.2	388.6	581.4	771.8
Ta	0.5	1.7	1	1.4	1
Th	1.1	7	2.3	3.6	3.8
U	0.4	1.6	0.5	0.7	0.6
V	306	244	259	306	266
Zr	92.2	207	93	128.3	98.5
Y	27.4	37	19.7	26.3	22.5
La	11.6	24.7	16.6	23	25.7
Ce	23.3	52.4	31.6	48.7	53.2
Pr	2.96	5.89	3.7	5.26	5.65
Nd	14	22.6	14.8	19.5	19.8
Sm	3.29	5.29	3.27	4.34	4.1
Eu	1.2	1.71	1.13	1.58	1.24
Gd	4.19	6.26	3.6	4.81	4.35
Tb	0.77	1.1	0.63	0.81	0.7
Dy	3.96	6.05	3.63	4.43	3.93
Ho	0.99	1.4	0.81	1.05	0.82
Er	2.85	3.91	2.34	2.77	2.34
Tm	0.39	0.6	0.35	0.42	0.32
Yb	2.65	3.85	2.04	2.42	2.04
Lu	0.38	0.55	0.29	0.4	0.31
Mo	0.2	0.5	0.9	0.6	0.4
Cu	101.5	68.6	78.1	111.1	116.6
Pb	311.1	2.8	160.8	2.7	221.4
Zn	238	74	269	68	410

LOI = Loss On Ignition; Mg# = Mg number.

* Total iron as Fe_2O_3.

Kuristyk basalts, low to moderate Ni–Cr concentrations, and Al_2O_3 contents around 14–16 wt.% (Table 3; Fig. 8A). Their major element composition is close to that of N-MORB and continental thoeliitic basalts except for CaO, which varies from 6–8 to 12–14 wt.% (Fig. 8B), likely due to variable alteration, particularly in sample TZ16, where calcite occurs as pseudomorph on plagioclase phenocrystals. In a silica versus alkali diagram (Fig. 8D), samples TZ8-9 and TZ16-17-19 show a trend that follows the alkaline picrobasalt-to-trachybasalt series but this could be due to an excess of Na_2O given by alteration of plagioclase. For this reason, we plotted relatively immobile elements such as Zr, Y and Nb in tectonomagmatic discrimination diagrams portrayed in Fig. 8E and F, where the analyzed rocks can be classified as within-plate tholeiitic to transitional basalts. This is confirmed by the trace elements composition, reported in Table 3 and portrayed in Fig. 9.

The Primitive Mantle normalized (PM) Rare Earth Element (REE) compositions of the Shindy Basalts are shown in Fig. 13A. All samples display rather flat Medium- and Heavy-REE patterns

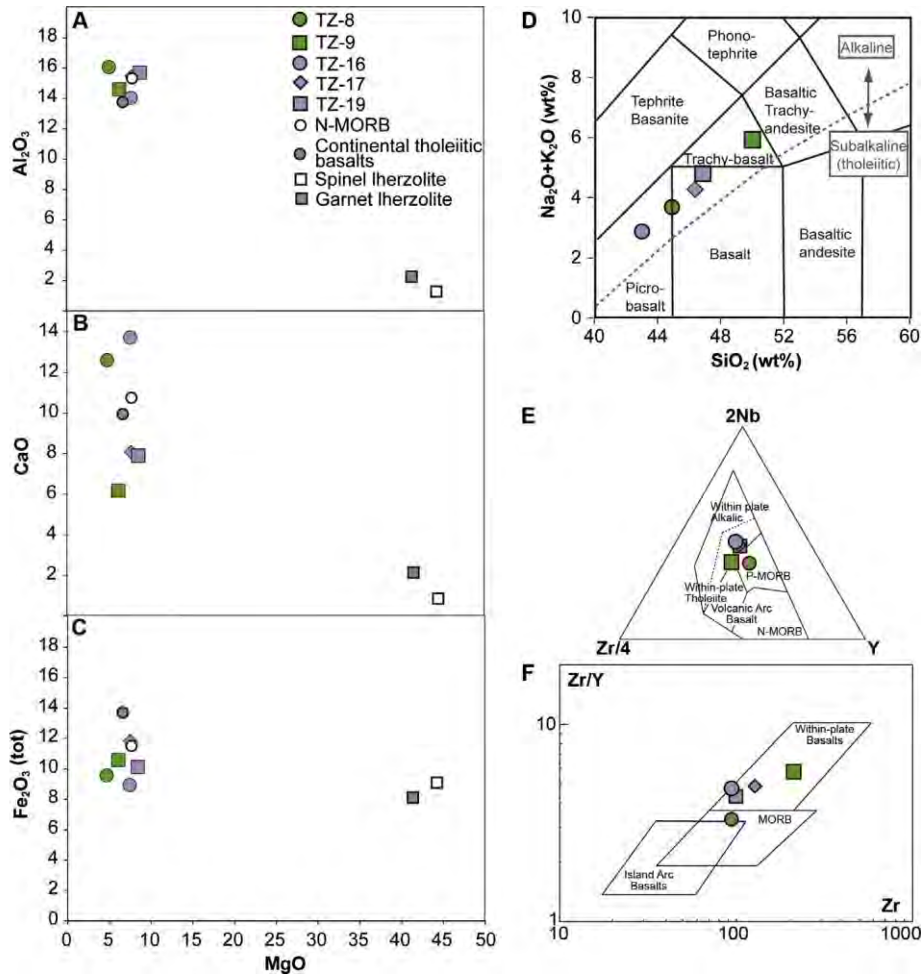

Fig. 8. (A–C) Bulk-rock major element compositions of Shindy basalts compared with average Normal-MORB (Hofmann, 1988), average Continental Tholeiitic Basalts from Deccan province (Peng et al., 1998; Lightfoot et al., 1990; Crocket and Paul, 2004) and average spinel- and garnet lherzolites (McDonough, 1994). (D) Total alkali elements versus wt.% SiO_2. Dashed line separating alkaline from subalkaline (tholeiitic) basalts is from Irvine and Baragar (1971). (E) 2Nb-Zr/4-Y tectonomagmatic discrimination diagram for basaltic rocks (after Meschede, 1986). (F) Zr–Zr/Y diagram after Pearce and Norry (1979).

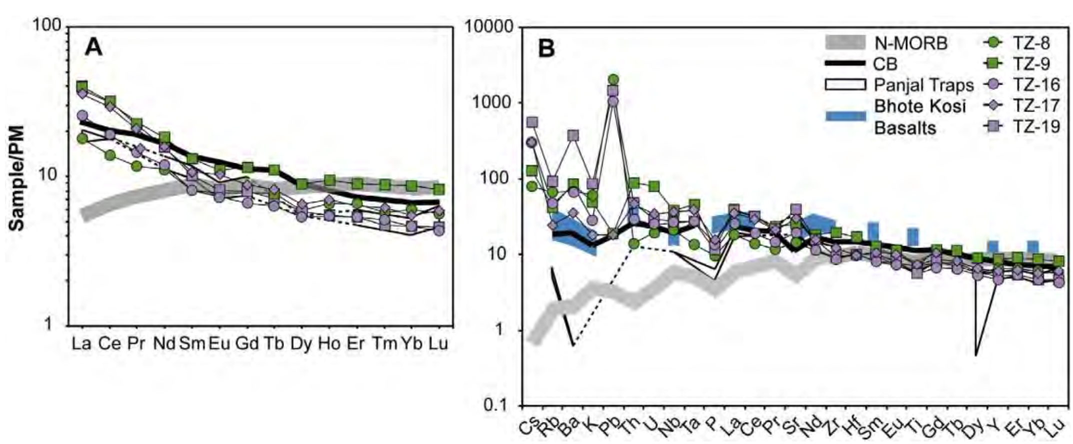

Fig. 9. Primitive mantle normalized REE (A) and other trace element (B) concentrations of Shindy basalts. Shaded gray area represents average N-MORB pattern (Hofmann, 1988); the black solid line is the average pattern of continental tholeiitic basalts. from Deccan province (Lightfoot et al., 1990; Peng et al., 1998; Crocket and Paul, 2004), the white and blue areas are the composition of Panjal Traps (Vannay and Spring, 1993), and Bhote Kosi basalts (South Tibet; Garzanti et al, 1999), respectively. Normalizing values after McDonough and Sun (1995). Elements are presented in order of increasing compatibility (left to right) during melting in the upper mantle (Hofmann, 1988; Sun and McDonough, 1989). Abbreviations: CB = continental tholeiitic basalts.

with absolute concentrations at 10 PM, while Light-REEs reach average of tholeiitic basalts with continental affinity (CB) from values up to 40 PM with a pattern comparable with that of an the Deccan province, India (Lightfoot et al., 1990; Peng et al.,

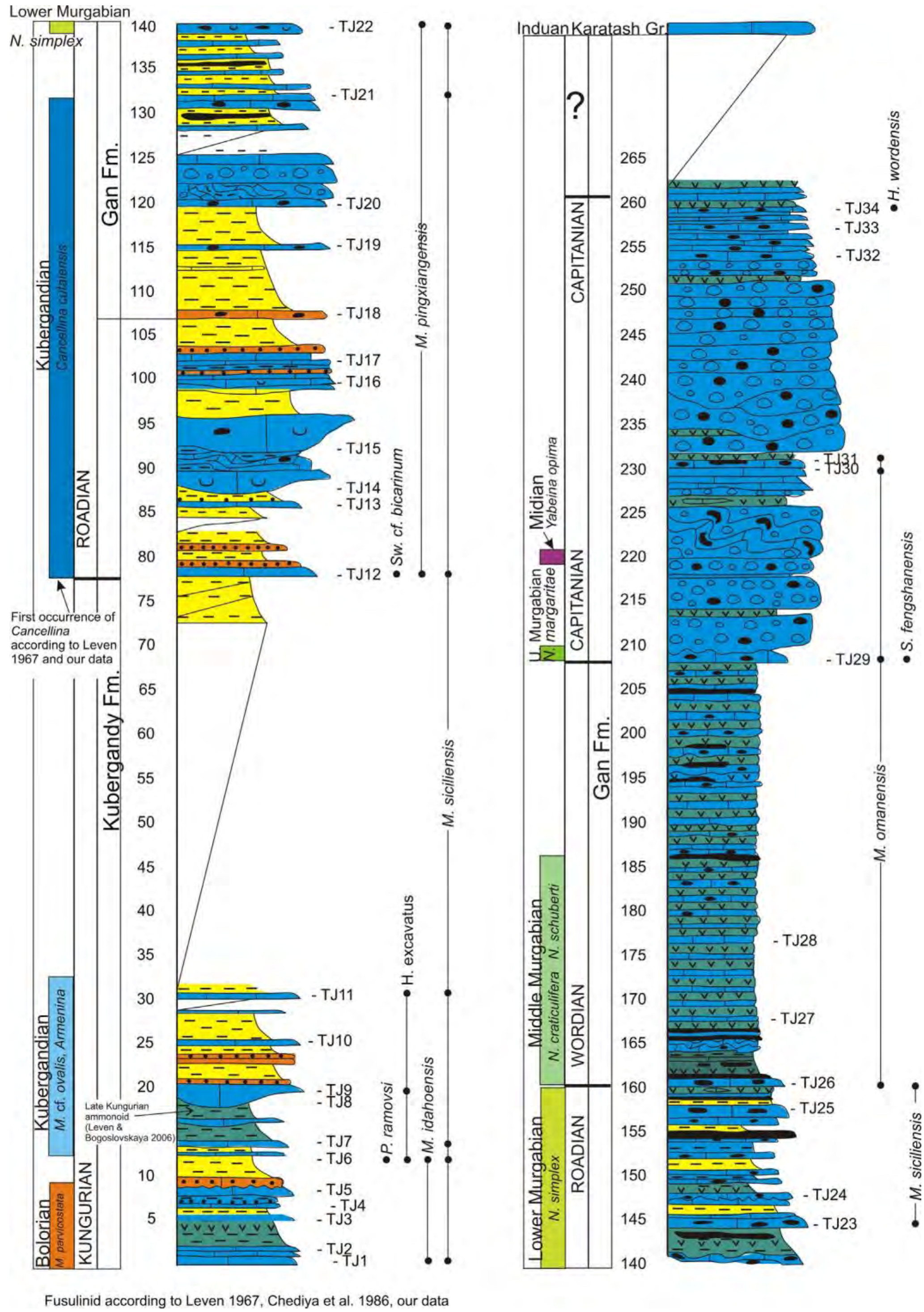

Fig. 10. Kubergandy type-section. Base: 3752^{0}04.4^{00}N–7337^{0}19.4^{00}E; 3950 m a.s.l. Base of conglomerate: 3751^{0}57^{00}N–7337^{0}26.2^{00}E; 4026 m a.s.l. S0: 163/55. Legend as Fig. 5. Only the most significant condont and fusulinid taxa a reported. For the complete list see Table 2a–2c.

1998; Crocket and Paul, 2004). The full spectrum of analyzed trace elements (REE; Large Ion Lithophile Elements, LILE and High Field Strength Elements, HFSE) is shown in Fig. 9B and is compared with the reference Mid Ocean Ridge Basalt (MORB; Hofmann, 1988) and CB. As a whole, the Shindy Basalts from both Mudzubulak and Kuristyk localities fit rather well with the CB pattern (black line in Fig. 9B) for a large number of elements measured, particularly for the fluid-immobile elements like Nb, Ta, Zr, Hf, and Ti (HFSE), HREE and Sc. They are instead more enriched in fluid-mobile elements, with spikes of Cs, Ba, Pb (LILE), and a positive anomaly in Sr, As for some major elements, this could be due to a subsequent alteration (or a crustal contamination).

4.3. Fossil content

The Kochusu Formation contains fusulinids [Monodiexodina shiptoni (Dunbar) and species of Chalaroschwagerina, Darvasites, and Leeina] (e.g. Gaetani and Leven, 2014), smaller foraminifers (Multidiscus sp.), algae, brachiopods, ammonoids, rare rugose corals, and conodonts. Ammonoids and rugosa also occur among pillow lavas in the Shindy Formation.

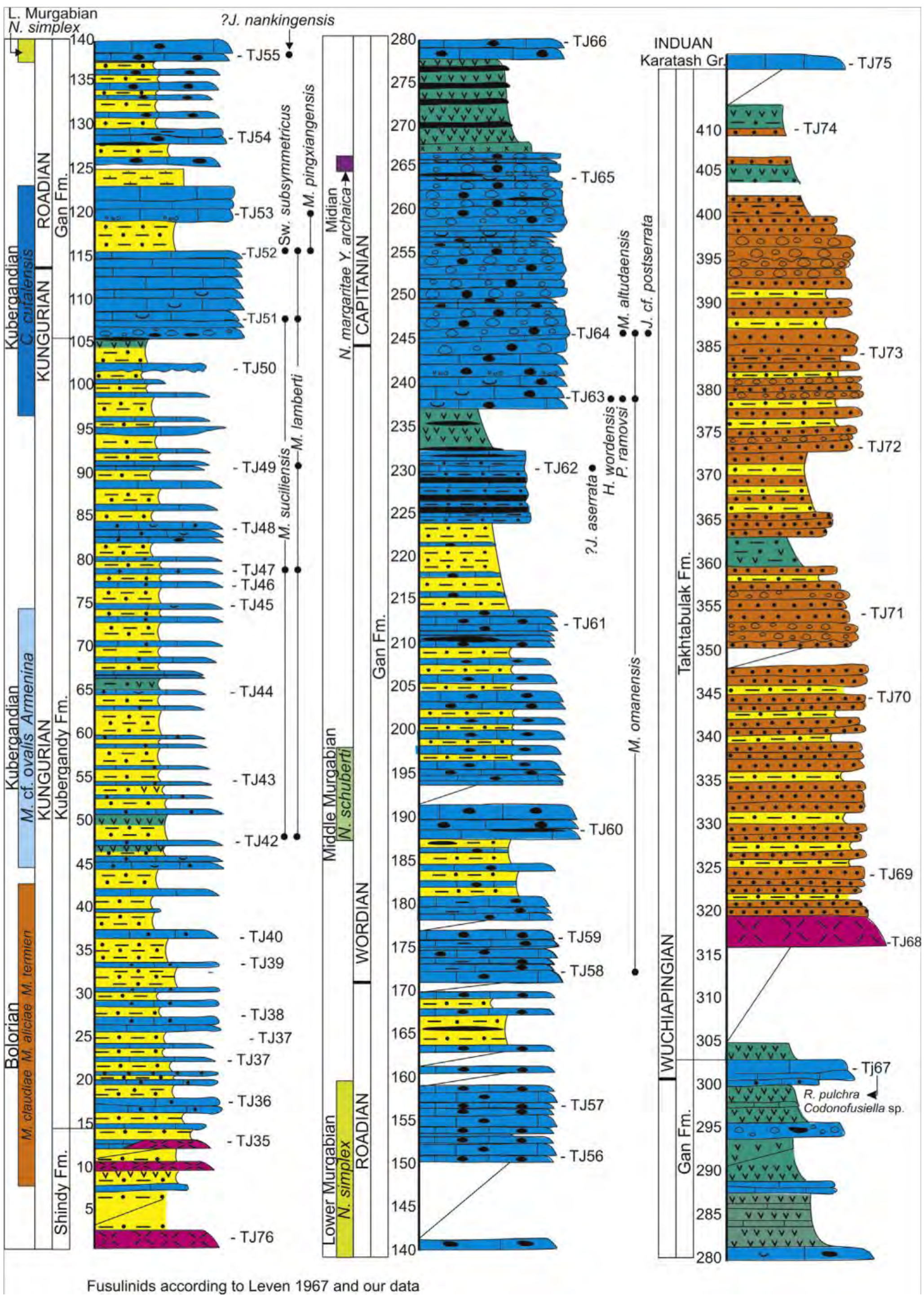

Fig. 11. Kutal 2 section. Base: 3805^{0}10.4^{00}N–7358^{0}22.4^{00}E; 3974 m a.s.l. S0: 350/60. Legend as in Fig. 5. Only the most significant conodont and fusulinid taxa are reported. For the complete list see Tables 2a–2c.

4.4. Age

According to several authors (Leonova and Dmitriev, 1989; Leven et al., 1989; Reimers, 1999; Kozur, 1994), ammonoids and conodonts suggest a Bolorian (latest Early Permian) age for the Shindy and Kochusu formations, correlatable to the Kungurian of the International (Global) Scale (Gaetani and Leven, 2014).

5. Kubergandy Formation

The Kubergandy Formation was established by Dutkevich (1937). The Kubergandy type section (Fig. 6D) is very important because it is the stratotype for the Kubergandian Stage of the Tethyan Scale (Leven, 1967, 1981). We have measured and sampled two detailed stratigraphic sections in the Kubergandy Formation: the Kubergandy type section and the Kutal 2 section (Figs. 10 and 11) for a thickness of respectively 105 and 107 m.

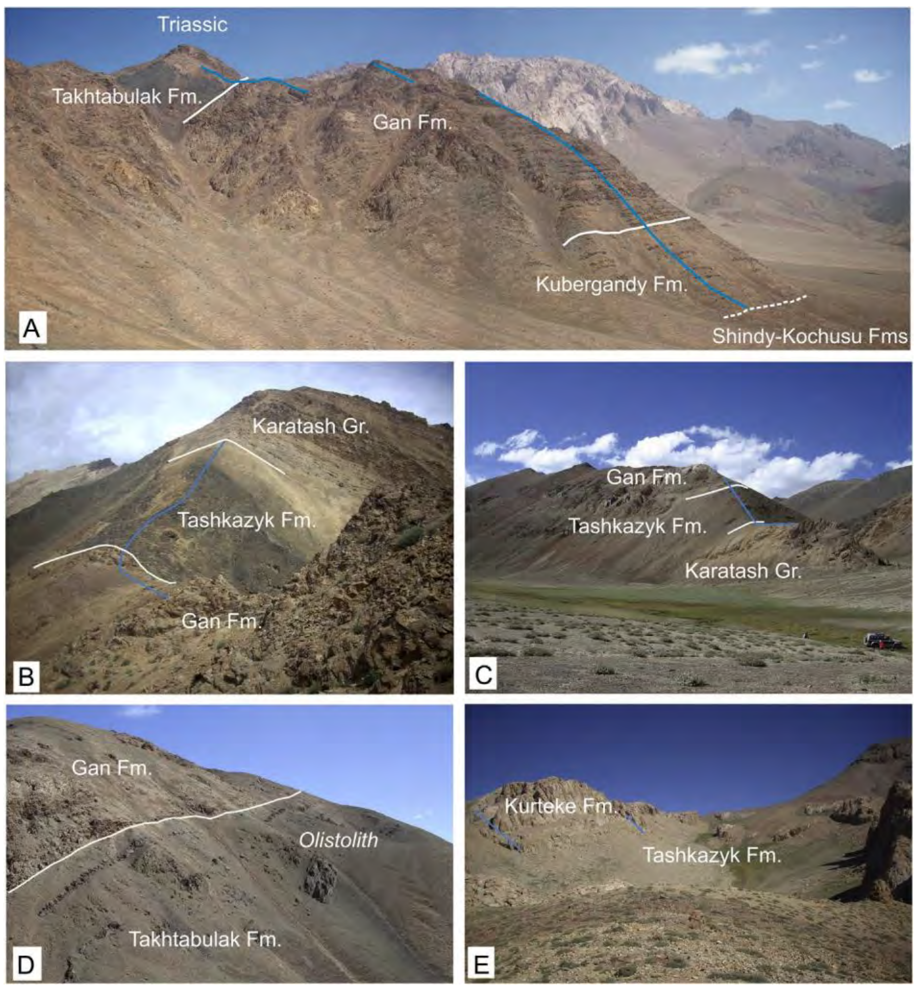

Fig. 12. (A) Photo of the Kutal 2 section ($3805^{0}10.4^{00}$N–$7358^{0}22.4^{00}$E; 3974 m a.s.l.). (B) Photo of the Kutal 2 section. Upper part showing the Karasin Member in the foreground and the Takhtabulak and Karatash formations in the background. (C) photo of the Kuristyk section. ($3748^{0}23.5^{00}$N–$7423^{0}21.2^{00}$E; 4317 m a.s.l.). (D) Olistoliths in the upper part of the Takhtabulak Formation on the slope in front of the Kuristyk section. (E) photo of the Kurteke 1 section ($3749^{0}51.2^{00}$N–$7402^{0}20.6^{00}$E; 4317 m a.s.l.).

5.1. Lithology

The Kubergandy Formation comprises bioclastic calcarenites, calcareous siltstones and sandstones and dark shales with a few volcaniclastic sandstones and intercalations of volcanic ashes.

In the lower part, shales are dominant, and graded calcarenites and subordinate hybrid sandstones form planar to lenticular 20– 50 cm-thick beds (Supplementary Fig. S2). In the upper part, calcarenites increase in frequency and thickness (Supplementary Fig. S2), forming m-thick channelized bodies with coarser grained texture.

Microfacies analysis shows that the limestones mainly consist of bioclastic packstones with fusulinids, smaller foraminifers, algae, echinoderms, brachiopods, and bivalves.

The limestones and the calcareous sandstones show neat sedimentary structures as cross-, convolute- and parallel laminations and gradation; beds with erosional base, channelized bodies and slumpings occur interbedded within the shales.

5.2. Fossil content

The formation was reported to contain fusulinids and ammonoids and to comprise three biozones: the Misellina parvicostata zone, the Misellina ovalis-Armenina biozone and the Cancellina cutalensis biozone (Leven, 1981; Chediya et al., 1986). We have found fusulinids, foraminifers and conodonts, as reported in Tables 2a and 2b and Supplementary Figs. S3–S6. Fusulinids are mainly represented by Misellina termieri, Misellina sp., Neofusulinella ex gr. giraudi, Parafusulina cf. dzamantalensis, Yangchienia cf. compressa and primitive species of Cancellina). The majority of the smaller foraminifers (neoendothyrins, palaeotextulariids, globivalvulinids, miliolates and nodosariates) are well known, but the FO (first occurrence) of Dagmarita, Graecodiscus, and Retroseptellina? is noticeable. There are also interesting dasycladaleans (Gyroporella? sp., Velebitelleae gen. sp.), algospongia (Efluegelia johnsonii, Stacheoides sp.), classical microproblematica (Archaeolithoporella hidensis and Tubiphytes obscurus), echinoderms, brachiopods, bivalves. Conodonts comprise Hindeodus wordensis, Mesogondolella idahoensis, M. lamberti, M. pingxiangensis, Pseudohindeodus ramovsi, Sweetognathus fengshanensi, and S. subsymmetricus. Deep-water ostracods are also present.

5.3. Age

According to Leven (1981) and Chediya et al. (1986), the lower part of the formation contains fusulinids of late Bolorian age; fusulinids and ammonoids in the middle and upper parts of the Kubergandy Formation characterize the Kubergandian Stage, with ammonoids in particular correlating with the assemblages of the Roadian stratotypes (see discussion in Leven and Bogoslovskaya, 2006). Generally, our samples are poor in fusulinids with only Schubertella sp. in TJ3–5 in the type-section and in TJ36 in the Kutal 2 section. However, our samples TJ37 and TJ38 from this latter

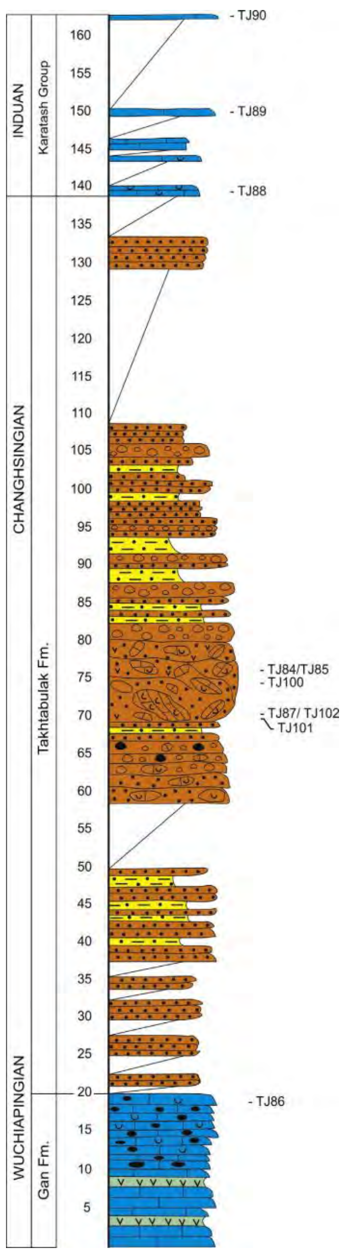

Fig. 13. Kuristyk section. Base: 3748^{0}23.5^{00}N–7423^{0}21.2^{00}E; 4317 m a.s.l. S0: 145/ 65. Legend as Fig. 5.

section contain Misellina spp., typical of the late Bolorian and confirm that the base of the Kubergandy Formation is still Bolorian in age. Parafusulina sp. and N. cf. giraudi in TJ8 indicate a Kubergandian age. The upper part of the formation (samples TJ12 to TJ17) contains evolved species of Cancellina and thus corresponds to the upper Kubergandian. So based on the Tethyan scale, the formation is late Bolorian to late Kubergandian.

Conodonts suggest a Kungurian age for the base of the formation, and an early Roadian age for sample TJ12 in the upper part of the formation at the type section based on the occurrence of Mesogondolella pingxiangensis (Ning et al., 2010). The top of the Kubergandy Formation seems to be younger in the Kubergandy section than in the Kutal 2 section where it still lies in the Kungurian, suggesting local diachroneity as would be expected for a formation boundary.

Thus, based on conodonts (Mei and Henderson, 2001, 2002; Henderson and Mei, 2003, 2007), most of the Kubergandy Formation was deposited in the Kungurian, reaching the early Roadian only in its upper part in the Kubergandy type section.

5.4. Palaeoenvironment

Sedimentary structures (laminations and gradation; beds with erosional base, channelized bodies and slumpings) indicate that the formation was deposited below the storm wave base down a slope. Microfacies analysis of the calcarenitic beds confirms this interpretation, as they consist of coarse bioclastic packstones with transported foraminifers, undetermined bioclasts and algal lumps, which are all highly abraded and fragmented indicating they were transported and resedimented along the slope from a nearby carbonate platform. They are mixed with an autochthonous fauna of bivalves, brachiopods, echinoderms and nodosariate foraminifers, which are typical of slope settings.

6. Gan Formation

The Gan Formation was introduced by Leven (1958) for a succession of turbiditic and micritic limestones and cherty siltstones. The formation was traditionally divided into several units: Agalkhar, Dhzamantal, Deire, Karasu and Kutal, already recognized by Dutkevich (1937).

We have measured and sampled two detailed stratigraphic sections in the Gan Formation: the Kubergandy type section and the Kutal 2 section (Figs. 11 and 12A and B) for a total thickness of 154 and 198 m respectively. The latter section is very close to the Dzhamantal section, the lectostratotype for the Murgabian Stage of the Tethyan Scale (Leven, 1967, 1981), which however was discarded in our fieldwork because strongly affected by faults and folds.

The boundary with the underlying Kubergandy Formation is drawn at the appearance of diffuse chert nodules. We do not follow the subdivision of the formation into members, as there is a considerable lateral lithological variability. Distinctive are however the breccias and conglomerates (Karasu Member) at the top of the formation (Fig. 12A and B, Supplementary Fig. S2).

6.1. Lithology

The lower part of the formation consists of cherty bioclastic limestones (mostly fine calcarenites) (Supplementary Fig. S2), cherts and greenish shales with a greater amount of volcaniclastic ashes with respect to the underlying formation; intercalation of conglomerates, channelized beds and slumpings occur.

The middle part of the formation is dominated by colored volcaniclastic ashes interbedded with thin-bedded nodular limestones and cherts (Supplementary Fig. S2). This unit is more evident in the Kubergandy section than in the Kutal 2 section.

Two distinct microfacies were recognized in the limestones: (1) a microfacies of bioclastic packstones, finer than those of the Kubergandy Formation, containing foraminifers, peloids, thin-shelled bivalves, and echinoderms; (2) a microfacies of wackestones/packstones with radiolarians, sponge spicules and thin-shelled bivalves.

The upper part of the formation consists of very thick polymict conglomerates and breccias (Supplementary Fig. S2), which are clast-supported, immature, poorly sorted, with both spherical and elongate, rounded and angular 3–40 cm-wide clasts of cherts, limestones, and volcaniclastic rocks. In the lower part of the unit, the conglomerates form lenticular bodies with erosive bases, which cannibalize each other; in the upper part, they are better organized in metre-thick beds. Sporadic intercalations of volcaniclastic ashes, thin-bedded limestones (wackestones with radiolarians, sponge spicules and pelagic bivalves) and slumpings are also present. In the Kutal 2 section, the conglomerates are less thick and the Gan Formation ends with about 30 m of cherty bioclastic limestones (calcarenites and calcirudites; subordinate calcilutites) and volcaniclastic ashes.

6.2. Fossil content

The Gan Formation is characterized by the occurrence of fusulinids, foraminifers, algae (Permocalculus sp.), pelagic bivalves, ostracods, echinoderms and Tubiphytes ex gr. obscurus.

Leven (1967) and Chediya et al. (1986) reported the occurrence of fusulinids – scantly present in the upper part – from the Gan Formation both along the Kubergandy and the Kutal 2 sections, among which species of Armenina, Praesumatrina, Verbeekina and Neoschwagerina simplex in the lower middle part of the formation, N. schuberti, N. ex gr. craticulifera, Sumatrina brevis and species of Afghanella, Armenina, and Verbeekina about 10–15 m above, and Dunbarula ex gr. schubertellaeformis, N. ex gr. margaritae, and S. annae at the base of the conglomerates. Finally, they reported primitive Yabeina (Y. ex gr. opima and Y. archaica, two species which are probably synonymous) and species of Lantschichites, Neoschwagerina, and Yangchienia from the conglomerates.

According to our data (Tables 2a–2c, Supplementary Figs. S4 and S6–S8), fusulinids and foraminifers at the base of the Gan Formation in the Kutal 2 section comprise Climacammina sp., Endothyra sp., Eotuberitina reitlingerae, Geinitzina aff. spandeli, Globivalvulina sp., Hemigordiellina sp., Pachyphloia ovata, Polytaxis sp., Postendothyra sp., Pseudodoliolina? sp., and Schubertetella ex gr. melonica; at the top they include Bidagmarita sp., Codonofusiella sp., Globivalvulina sp., Midiella sp., Multidiscus? sp., Neogeinitzina sp., Pachyphloia ovata, Rectostipulina quadrata, and Reichelina pulchra.

We also found conodonts as reported in Tables 2a and 2b. In the Kubergandy section, conodonts at the base (samples TJ21-22) comprise Mesogondolella pingxiangensis, M. siciliensis, and transitional forms Sweeetognathus guizhouensis-S. subsymmetricus; at the top (TJ34) Hindeodus wordensis and M. altudaensis. In the Kutal 2 section conodonts at the base (sample TJ51) comprise M. lamberti, M. siciliensis, and transitional forms S. guizhouensis – S. subsymmetricus; at the top (samples TJ63-64): H. wordensis, M. altudaensis, M. omanensis, M. cf. postserrata, and Pseudohindeodus ramovsi.

6.3. Age

The lower-middle part of the formation was considered to be Murgabian to Midian in age by Chediya and Davydov (1980) and Chediya et al. (1986). The breccias and conglomerates (Karasu Member), being poor in fusulinids, were conventionally placed in the Midian, even if a Late Permian age was not excluded (Leven, 1998). So, in terms of the Tethyan regional scale, it ranges from the Murgabian to the early Dzhulfian.

Newly recovered conodonts at the base of the formation in the Kutal 2 section suggest a Kungurian age (Henderson and Mei, 2003; Ning et al., 2010; Reimers, 1991), whereas those reported from the Karasu member are Capitanian (Mei and Henderson, 2001). The Gan Formation in the Kubergandy section covers a narrower age, starting already in the Roadian and ending in the Capitanian (Henderson and Mei, 2003; Kozur, 1994; Kozur and Wardlaw, 2010 Reimers, 1991).

Also, in the Kutal 2 section, the fusulinids Reichelina and Codonofusiella and the smaller foraminifers Rectostipulina and Bidagmarita, from the very top of the Gan Formation, above the Karasu breccias and conglomerates, indicate a Wuchiapingian age. So, the overall range of the Gan Formation stretches from the late Kungurian to the early Wuchiapingian.

6.4. Palaeoenvironment

The facies of the Gan Formation indicate deposition and resedimentation along a slope, but in a more distal setting than that recorded by the underlying Kubergandy Formation, and a remarkable increase in volcanic activity. As in the Kubergandy Formation, the metazoan fragments, the fusulinids and the conodonts are highly abraded and fragmented, indicating considerable transport. Also the ostracods are mainly deep water species (S. Crasquin, pers. comm.).

The maximum depth is recorded by the radiolarian and sponge wackestones intercalated to cherts and colored volcaniclastic ashes, just below the conglomerates.

The thick conglomerate bodies indicate a marked reprisal of tectonic activity possibly related to syn-depositional block faulting and formation of debris flow along steep fault scarps, during a major regression, which occurred at the end of the Capitanian.

They are thus correlatable to similar debris flows, which occur in the late Middle Permian Kundil Formation of Karakorum, Pakistan (Gaetani et al., 1995). This suggests that this tectonic activity coupled with regression is a global event recognizable in the most of the Cimmerian blocks.

7. Takhtabulak Formation

The Takhtabulak Formation was established by Dutkevich (1937) and later subdivided into three units by Grunt and Dmitriev (1973).

We have measured and sampled two detailed stratigraphic sections in the Takhtabulak Formation: the Kutal 2 section and Kuristyk section (Figs. 11, 12B and C and 13) for a total thickness of 110 and 119 m, respectively. The Takhtabulak Formation was also studied and sampled at Mudzubulak.

The boundary with the underlying Gan Formation has been drawn at an ash bed (frequently covered) which marks the disappearance of limestones. In the Kutal 2 section, the formation starts with a huge olistrostrome enclosing metre-sized boulders of basaltic lavas and limestones (Supplementary Fig. S2) covered by green volcaniclastic sandstones, whereas in the Kuristyk section, the base of the formation consists of volcaniclastic sandstones.

7.1. Lithology

Most of the formation is made of dark green volcaniclastic sandstones (Supplementary Fig. S2), shales and subordinate conglomerates, with sedimentary structures as parallel lamination and gradation; rare intercalations of sandy calcarenites occur. Sandstones are dominated by mafic volcanic detritus including abundant basalt grains and lathwork rock fragments (Lv 97 ± 3, Vm/V 79 ± 4; Table 1).

At the base of the formation in the Kutal 2 section, metre-sized boulders of basaltic lavas and limestones are embedded in volcaniclastic sandstones.

In the middle part of the formation in the Kuristyk section and at Mudzubulak, metre-sized boulders of stratified bioclastic limestones and algal, coral, and sponge biostromes occur.

Microfacies of bioclastic limestones reveal coarse packstones with fusulinids, rugosa and tabulate corals, sphinctozoans, brachiopods, echinoderms, ostracods and carbonate and volcanic extraclasts.

7.2. Fossil content

The intercalation of bioclastic limestones and the boulders of coral-sponge-bryozoan bioconstructions embedded in the formation contains a very rich biota of fusulinids (Reichelina pulchra), smaller foraminifers, algae, brachiopods (Anchorhynchia sarciniformis, Costisteges sp. ind., Enteletella nikschitshi, Enteletes dzaghrensis, E. meridionalis, Heterelasmina lepton, Martinia bisinuata, M. aff. warthi, M. rupicola, M. sp. 1, M. sp. 2., Notothyrina pontica, Notothyris pseudodjoulfensis, Orthothichia avushensis, Parenteletes ruzhencevi, Paramarginifera sp. ind., Streptorhyncus aff. pelargonatus, and Stenoscisma armenica), bivalves, echinoderms, bryozoans, tabulate and rugosa corals and sponges (sphinctozoans) (Table 2c, Supplementary Fig. S9).

7.3. Age

According to Grunt and Dmitriev (1976), fusulinids and brachiopods in the lower part of the formation suggest a late Dzhulfian-early Dorashamian (Late Permian) age, which is in agreement with our finding that the top of the underlying Gan Formation is early Late Permian (Wuchiapingian). According to Leven (1998), Colaniella parva and Palaeofusulina aff. fusiformis occur at the base of the Takhtabulak Formation. If these determinations were correct, then the age of the Takhtabulak Formation would be Changhsingian also at its base. However, these specimens are not figured in Leven (1967, 1998), so it is not possible to confirm their taxonomic determinations, as we have not found any in our sections.

The conodont Clarkina subcarinata (Sweet) was found in the upper part of the formation by Kozur (1994), indicating a Changhsingian age. Thus, the formation is here considered to span the Wuchiapingian-Changhsingian.

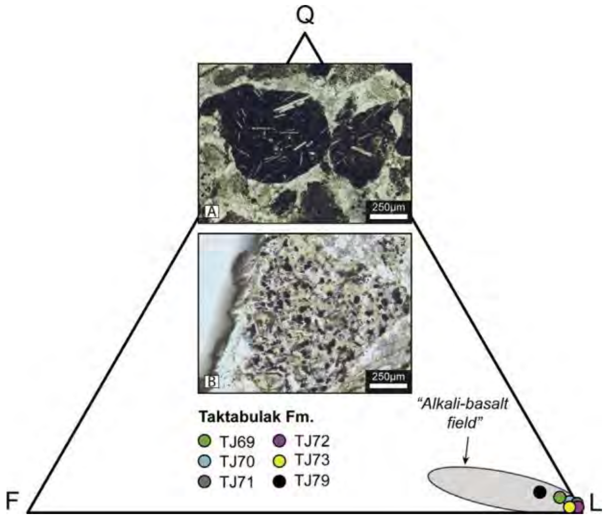

7.4. Palaeoenvironment

The pure volcaniclastic composition, recorded by the detrital modes of the Taktabulak Formation, attests to erosion of a mafic volcanic edifice (Fig. 14. ''Volcanic rifted-margin provenance''; Garzanti et al., 2001).

Sedimentary structures in the volcaniclastic sandstones and conglomerates are also indicative of resedimentation along a slope. Tectonic activity should have been intense, with slope instabilities causing resedimentation of meter-sized olistoliths of bioclastic limestones, biostromes and basaltic lavas. There are several features, which suggest that both the bioclastic limestone boulders and the bioconstructions are olistoliths transported along the slope. The limestone boulders are in fact stratified obliquely to the S0 of the formation (Fig. 12D). The build-ups are not growing on the sandstones of the slope as suggested by Grunt and Dmitriev (1973), as most reefal organisms are in life position but they are discordant to the stratigraphic polarity of the succession.

8. Kurteke Formation

The Kurteke Formation was introduced by Leven (1967) for a succession of bioclastic and massive microbialitic and coral

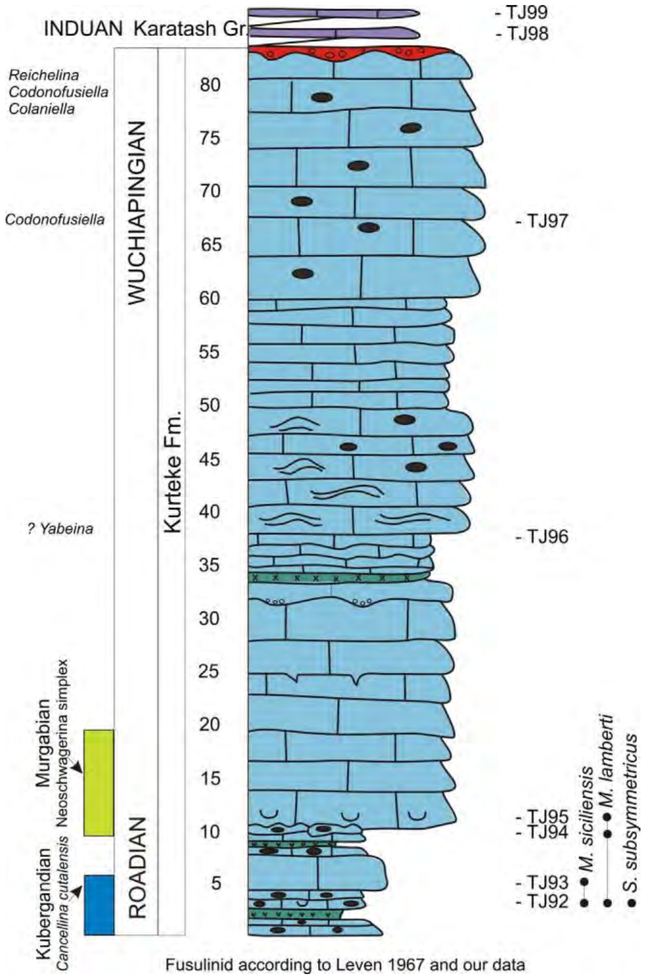

Fig. 14. Volcanic detritus from the Taktabulak Formation (''Undissected volcanic provenance'' by Garzanti et al., 2001). (A) Basaltic grains (sample TJ71). (B) Intergranular lathwork volcanic grain (sample TJ73). Alkali-basalt field by Garzanti et al., 2001.

Fig. 15. Kurteke 1 section. Base: 3749^{0}51.2^{00}N–7402^{0}20.6^{00}E; 4317 m a.s.l. Legend as Fig. 5.

limestones, which was lying at the core of horseshoe arranged palaeogeographic domains (Leven, 1967, Fig. 1), surrounded by the deeper water settings described above.

We have measured the Kurteke 1 section at Kurteke (3749^{0}51.2^{00}N–7402^{0}20.6^{00}E; 4317 m a.s.l.) on the right hydrographic side of the valley which is the second left inflow of the Kurteke River (type section of Leven, 1967) (Figs. 12E and 15). The total thickness of the formation is 86 m. At Kurteke 1, the base is not exposed, the talus covering the very few and scanty outcrops of the Tashkazyk Formation, which however is reported as outcropping by the Russian authors.

We observed the lower part of the Kurteke Formation also at Mamasar Bulak (3753^{0}03.5^{00}N–7351^{0}58.8^{00}E), along the Pamir highway.

8.1. Lithology

The lower part of the Kurteke Formation consists of partly covered red bioclastic limestones with crinoids and fusulinids, which crop out discontinuously; they pass to 15–25 cm-thick cherty bioclastic calcarenite beds with rare volcaniclastic ashes. These grade in turn to massive limestones locally microbialitic, becoming more bioclastic towards the top. At the top, the massive limestones are eroded by a laterally discontinuous conglomerate and pass to a mostly covered succession which according to the Russian authors (e.g. Leven, 1967; Chediya and Davydov, 1980; Grunt and Dmitriev, 1973) contains a laterite and then black limestones of Triassic age. This succession, however, is laterally cut by a thurst surface stacking the Gan Formation on top of the measured section. Along the thrust surface a foliated cataclasite is present.

At Mamasar Bulak, bioclastic calcarenites–calcirudites with crinoids, brachiopods, bryozoans and corals crop out below very recrystallized massive limestones.

Microfacies analysis shows that the formation comprises at the base grainstones and packstones with fusulinids, smaller foraminifers, echinoderms, brachiopods, algal lumps and bryozoans. The microfacies associated to the microbialites comprise peloidal packstones with brachiopods, whereas in the upper part there are again bioclastic packstones with fusulinids, smaller foraminifers, algal lumps, and echinoderms.

8.2. Fossil content

The formation contains fusulinids, smaller foraminifers, algae, echinoderms, brachiopods (species of the genera Martinia, Overtonina, Retimarginifera, Costiferina, Magniplicatina, Boloria, Labaia, and Spiriferella), bryozoans, and Tubiphytes sp. (Table 2c).

The conodonts Mesogondolella lamberti, M. siciliensis, and Sweetognathus subsymmetricus, were found in sample TJ92 at the base of the formation in a microfacies comprising Climacammina sp., Donezella hirtipes, Eotuberitina sp., Globivalvulina sp., Lasiodiscus tenuis, Mizzia? sp., Neoendothyra cf. staffelloides, Parafusulina? sp., Permocalculus? sp., Polytaxis? sp., Postendothyra sp., Schubertella sp., and T. obscurus (Supplementary Figs. S5 and S10).

Worthy of note is also the occurrence of Cancellina cutalensis in TJ93 and Neoschwagerina simplex, Parafusulina? cf. shakgamensis, Praesumatrina neoschwagerinoides, and Yangchienia sp. in samples TJ94-95 (Supplementary Fig. S10).

8.3. Age

Based on its fusulinid content, the Kurteke Formation was reported to span the Middle-Late Permian time interval by the Russian authors (Leven, 1967; Chediya and Davydov, 1980).

Our new data allow us to refine the age of the Kurteke Formation, especially the base, which is dated to the latest Kubergandian (TJ93) to earliest Murgabian (TJ94-95) by the fusulinids and to the latest Kungurian-early Roadian by the conodonts (Mei et al., 2002; Mei and Henderson, 2001). Consequently, this section is very interesting for discussing the chronostratigraphic correlations between the Tehyan regional stages Bolorian, Kubergandian and Murgabian and the standard stages Kungurian, Roadian and Wordian (see Section 10).

8.4. Palaeoenvironment

The Kurteke Formation represents several carbonate platform environments from the inner shelf with microbialites and peloidal packstones to higher energy platform margin settings where bioclastic shoals accumulated. Except for a few ash bed at the base, no volcanic layers have been recorded in the massive limestones of the Kurteke Formation, probably due to the unfavorable depositional conditions (i.e. high hydrodynamic energy, erosion).

9. Karatash Group

The Lower-Middle Triassic Karatash Group (up to 100 m-thick) comprises uniform thin-platy black to dark gray limestones (Kushlin, 1973). The Karatash Group of the Intermediate zone (sensu Dronov and Leven, 1960) is subdivided into the Bail'tam, Taldykol, and Zougan formations (Dronov and Luchnikov, 1976). It is considered to be Induan–early Anisian in age based on conodonts (Dagys and Dronov, 1989) and on the occurrence of the bivalve Claraia orientalis and the ammonoid Flemingites sp. which were found near its base (Grunt and Dmitriev, 1973). South-east of the studied area in the Central Zone sensu Dronov and Leven (1960), the group was divided into the Khan and Yulla formations by Korchagin (2008). The Yulla Formation is overlain by the massive reefal limestones of the Chontash Formation and by the cherts of the Karakungei Formation (Korchagin, 2008).

We have sampled platy dark limestones (calcilutites and oobiocalcarenites) at the base of the Karatash Group at the top of the Kubergandy, Kutal 2, Kuristyk and Kurteke sections (Figs. 10, 11, 13 and 15; Supplementary Figs. S4 and S10). Thin sections of the limestones at Kuristyk and Kurteke show that they are mainly ooid, oncoid and peloid packstones with subordinate intercalations of gastropod, ostracod and bivalve packstones with extraclasts (Supplementary Fig. S10). We have found only Merrillina? sp. A (see Orchard, 2007) at the base of the Karatash Group in the Kuristyk section (Supplementary Fig. S6), which suggests an Induan age, more precisely late Griesbachian.

The occurrence of Claraia sp. and ''Spirorbis'' phlyctaena confirms its Induan age.

10. Correlation of the Middle Permian Tethyan stages with the ISC stages

The sedimentary succession of SE Pamir contains several stratotypes of the Permian stages of the Tethyan regional chronostratigraphic scale, established by Leven (1980) and primarily based on fusulinids.

The Tethyan scale adopts the two lower stages Asselian and Sakmarian (lower Lower Permian) from the Ural scale (e.g. Ruzhentsev, 1954; Leven and Shcherbovich, 1978, 1980; Davydov, 1984; Leven et al., 1992). The two following stages Yakhtashian and Bolorian (upper Lower Permian) have stratotypes located in Darvaz, N Pamir, (e.g. Leven, 1979, 1980, 1981; Leven et al., 1983) which in the Carboniferous and in the Permian was lying along the Eurasian margin, on the northern side of the Palaeotethys (Vachard and Montenat, 1996; Angiolini et al., 2013a, 2013b).

The stratotypes of the Kubergandian (Leven, 1963, 1981) and Murgabian (Miklukho-Maklay, 1958; Leven, 1967, 1981) stages (Middle Permian) are located in SE Pamir (Fig. 1); during the Permian, these successions were part of the Cimmerian blocks on the southern margin of the Palaeotethys Ocean (Angiolini et al., 2013a, 2013b).

The upper three stages of the Tethyan scale, Midian (upper Middle Permian), Dzhulfian and Dorashamian (Upper Permian) were instead established in Azerbaijan (formerly, part of the Transcaucasia), at that time palaeoequatorial and part of the Cimmerian blocks.

Our analysis of the fusulinids and conodonts of the Kubergandian stratotype (Kubergandy section, Leven, 1963, 1981) and the Murgabian part of the Kutal 2 section – located next to the tectonically deformed lectostratotype of Dzhamantal (Leven, 1967, 1981) of SE Pamir provides a tool of correlation between the International (Global) and the Tethyan regional scales, which still remains unresolved, particularly for the Middle Permian (e.g. Leven, 2001; Leven and Bogoslovskaya, 2006). Our study (Fig. 16, Tables 2a–2c) shows that the Bolorian and the lower part of the Kubergandian (Armenina-Misellina ovalis biozone) correlate to the Kungurian; the upper Kubergandian (Cancellina cutalensis biozone) and the lower Murgabian (Neoschwagerina simplex – Presumatrina neoschwagerinoides biozone) correlate to the Roadian; the mid Murgabian [formerly N. craticulifera biozone in Leven (1967); then, Afghanella tereshkovae-Neoschwagerina deprati biozone in Leven (1992)] correlates to the Wordian; the upper Murgabian [formerly N. margaritae biozone; then Afghanella schencki-Neoschwagerina haydeni biozone (Leven, 1967, 1992)] and the lower Midian Yabeina archaica biozone correlate to the early Capitanian (Fig. 16).

Our proposed correlation of the upper Kubergandian-lower Murgabian to the Roadian – obtained using conodonts and fusulinids- supports the one previously suggested by Leven and Bogoslovskaya (2006) based on fusulinids and ammonoids. This correlation seems thus to be sound and reproducible. However, it contradicts Davydov et al. (2013, Fig. 5) who (1) suggest that the Bolorian corresponds to the latest Kungurian, (2) reduce the Bolorian to the Brevaxina biozone, and (3) remove the Misellina biozone (i.e., the late Bolorian-early Kubergandian interval). It is to be noted that the conclusions of Davydov et al. (2013) are mostly based on fusulinids from Darvaz, which was lying north of the Palaeotethys Ocean and thus belonged to a different palaeobioprovince than SE Pamir.

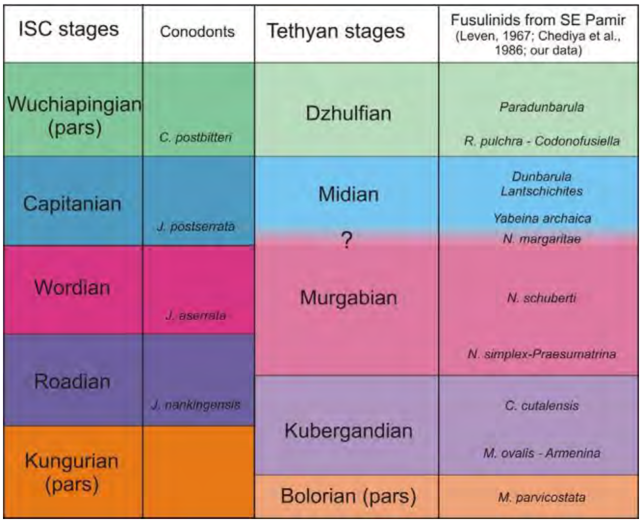

Fig. 16. Suggested correlation of the Middle Permian Tethyan stages in SE Pamir with the ISC stages. Position of taxa in the table do not correspond to their FADs.

Also, both our suggested correlations and those of Davydov et al. (2013) are not in agreement with the findings of Shen et al. (2013) in central Japan, who recovered lower Murgabian fusulinids (Cancellina nipponica, Neofusulinella praecursor, Neoschwagerina simplex) along with Kungurian conodonts (Hindeodus permicus, Meiognathus pustulus, Pseudohindeodus augustus, and Sweetognathus guizhouensis). The findings of Shen et al. (2013) seem to indicate that in Japan the base of the Roadian is higher than the Kubergandian-Murgabian boundary, and thus higher that what we are observing in SE Pamir. This suggests some degree of diachroneity of appearance of these taxa in different biofacies or palaeogeographic regions.

Our suggested correlation of the upper Murgabian-Midian to the Capitanian may appear in contradiction with previous findings that seem to support the correlation of the lower and upper Murgabian to the Wordian and the lower Midian to the upper Wordian of the Global scale (Angiolini et al., 2008, 2010; Henderson et al., 2012; Gaetani and Leven, 2014; Ebrahim-Nezhad et al., 2014; Colpaert et al., 2015, and references therein). However, our proposed correlation is based on the co-occurrence of Capitanian conodonts and N. margaritae below the FO of primitive Yabeina in the Kubergandy sections [our own data and those of Chediya et al. (1986)]. This correlation remains open to discussion as both in the Dzhamantal and Kutal sections, Leven (1967) recorded N. margaritae only with Y. archaica in the conglomerates and breccias of the Karasu Member. To make the situation more complex, the lower part of the Karasu Member is considered upper Murgabian by Leven (1967, 1981) and Chediya et al. (1986), but it is placed in the Midian by Leven (1998); to be reminded that the Karasu Member is Capitanian based on our conodont data.

If we consider also the successions of Central Iran (Abadeh: Kobayashi and Ishii, 2003; Rettori et al., unpublished data), NW Iran (Ebrahim-Nezhad et al., 2014), and Afghanistan (Vachard, 1980; Colpaert et al., 2015), it appears evident that the interval between the LAD of Neoschwagerina simplex and the FAD of Yabeina archaica must be accurately revised for the fusulinids and/or smaller foraminifers. The same holds true for the correlation with S China and Japan.

It is also clear that the successions of SE Pamir are not the best place where to establish a detailed reference fusulinid biozonation for the Murgabian (and the Midian), as shown by their scanty, discontinuous, problematic and not reproducible record, and their tectonic context. The Murgabian lectostratotype of Dzhamantal (Leven, 1967, 1981), besides being tectonically deformed, has a poor fusulinid record for the middle and upper Murgabian (see Leven, 1967, p. 26, Fig. 7) and the nearby Kutal 2 section, even if not affected by folds or faults, has very few fusulinids (our own data and Leven, 1967, p. 28, Fig. 9).

However, the Kubergandy stratotype shows a better fusulinid record and a good conodont coverage allowing correlation of its lower part to the Kungurian and its upper part to the Roadian
(Fig. 16).

Our conclusion on the correlation of the middle and upper Murgabian needs further testing and discussion. Provincialism and lack of previous detailed study mean that some aspects of correlation remain preliminary.

11. Backstripping and sedimentary evolution of the succession

The backstripping procedure, generally performed along vertical (i.e borehole) successions (e.g. Scheck and Bayer, 1999), is also applied to outcropping successions (e.g. Berra and Carminati, 2010) to reconstruct the total and tectonic subsidence of a specific part of a sedimentary basin.

The classical backstripping method (Sleep, 1971; Van Hinte, 1978; Sclater and Christie, 1980) first restores the original (uncompacted) thickness of the sedimentary units (from the oldest), gradually compacted in successive steps, by the deposition of the overlying units. Compaction occurring during burial is considered only depth dependent (Schmoker and Halley, 1982). The compaction is calculated by the exponential porosity-depth relation / = /0 expcy, where / is the porosity at depth y, /0 is the porosity of sediments at the surface and c is an empirically derived lithological coefficient.

At each decompaction time-step the position in depth of the base of the considered succession (or total subsidence) results from the sum of the decompacted thicknesses of deposited sediments, adding the corrections (positive or negative) for palaeobathymetry (the compaction of the unknown succession below the oldest unit has not been considered). To remove the isostatic subsidence (Airy-type isostasy) related to the sedimentary load, a backstripping procedure was applied in order to estimate the subsidence related to geodynamic processes.

The final curves (total and tectonic subsidence) do not consider eustatic corrections, due to the high uncertainties on the absolute amplitude of eustatic sea-level changes.

Decompaction parameters were defined following the approach of Hölzel et al. (2008) and Berra and Carminati (2010). As parameters are related to single lithologies (e.g. Sclater and Christie, 1980; Schmoker and Halley, 1982; Goldhammer, 1997), decompaction parameters were calculated by averaging the parameters of the single lithologies (defined according to the values summarized in Table 1 of Berra and Carminati, 2010) occurring in the unit according to their relative abundance (weighted average). The resulting curves (Fig. 17A and B) thus report the total subsidence, tectonic subsidence and bathymetry in the time interval covered by the studied succession in two positions in the basin, characterized by different units and depositional setting at specific stratigraphic intervals.

The first curve shown in Fig. 17A is based on the slope to basin succession cropping out along the Kubergandy, Kutal and Kuristyk sections and comprises the units from the Bazar Dara Group to the Gurumdi Group, including the Kubergandy, Gan and Takhtabulak formations. The second curve (Fig. 17B) is referred to the platform succession of the Kurteke area and includes the Kurteke Formation instead of the three units listed above (Fig. 3).

Both curves show a consistent increase in tectonic subsidence in the Early Permian; they have a characteristic concave-up profile,

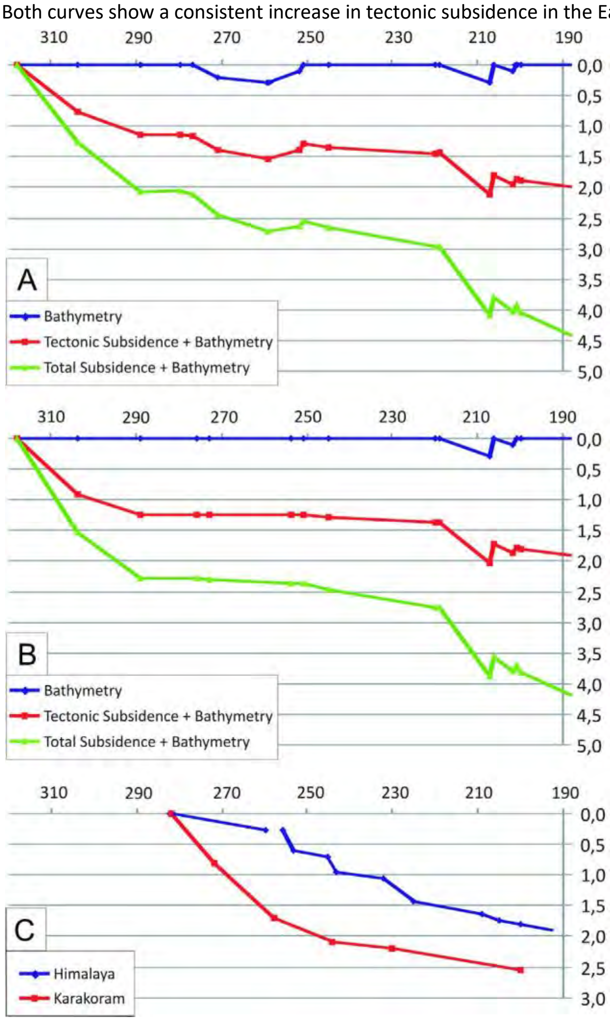

Fig. 17. Bathymetry, tectonic and total subsidence curves for (A) the slope-basinal succession (including Kubergandy, Gan and Taktabulak Fms) and (B) platform succession (including the Kurteke Fm.). For comparison, the total subsidence curves from Himalaya and KaraKoram (redrawn from Gaetani et al., 1990), covering partly the same stratigraphic interval, are reported (C). See also Fig. 3.

which is compatible with the structuration of a passive margin until the end of the Permian. The curve from the basinal succession suggests an increase in subsidence at the end of the Early Permian and in the Middle Permian. This increase in subsidence is reflected by the transition to deeper water facies, documenting that sedimentation was not able to keep pace with subsidence. The significance of this local change in subsidence (recorded both by the total and tectonic subsidence curves in Kubergandy, Kutal and Kuristyk) is not clear: the slight increase in tectonic subsidence in the basinal succession may be related to local block faulting. The return to shallower facies at the end of the Permian could be related to a possible, but not well-defined, tectonic uplift.

From the Early Triassic onward, the two curves show a trend reversal, their profile becoming clearly convex-up. The increase in tectonic subsidence, particularly evident in the Late Triassic, reflects an increasing subsidence with time, compatible with a progressive evolution from a passive margin to a peripheral foredeep setting, with a subsequent alternation of uplift and subsidence events. This part of the curve is explained by the collision of South Pamir and Central Pamir resulting in uplift and erosion of the Cimmerian collisional belt.

The subsidence curves obtained from the studied sections were compared with total subsidence curves from Karakoram and Himalaya sections published in Gaetani et al. (1990) that roughly cover the same stratigraphic intervals (Fig. 16C). The curve for the Himalayan succession is characterized by a highly irregular trend, which significatively differs from the SE Pamir curves. The Karakoram curve is instead very similar in its first part to the SE Pamir curves, suggesting a similar geodynamic control in the two domains (extensional margins). It is worthy of note that the passive margin trend in the Karakoram curve persists longer than in the Pamir curve, suggesting an older docking of the Pamir block to Eurasia with respect to Karakoram.

12. Geodynamic evolution and palaeogeographic implications

Angiolini et al. (2013a) showed that Karakoram, SE Pamir, Central Pamir and Qiangtang were part of a major Cimmerian belt which detached from Gondwana in the Early Permian. This belt was dissected into distinct terranes separated by extensional basins, as the Rushan ocean between Central and South Pamir (Leven, 1995), and the Wakhan Basin between Karakoram and South Pamir (Gaetani, 1997; Zanchi et al., 2000; Zanchi and Gaetani, 2011) (Fig. 18). Less clear are the possible correlations

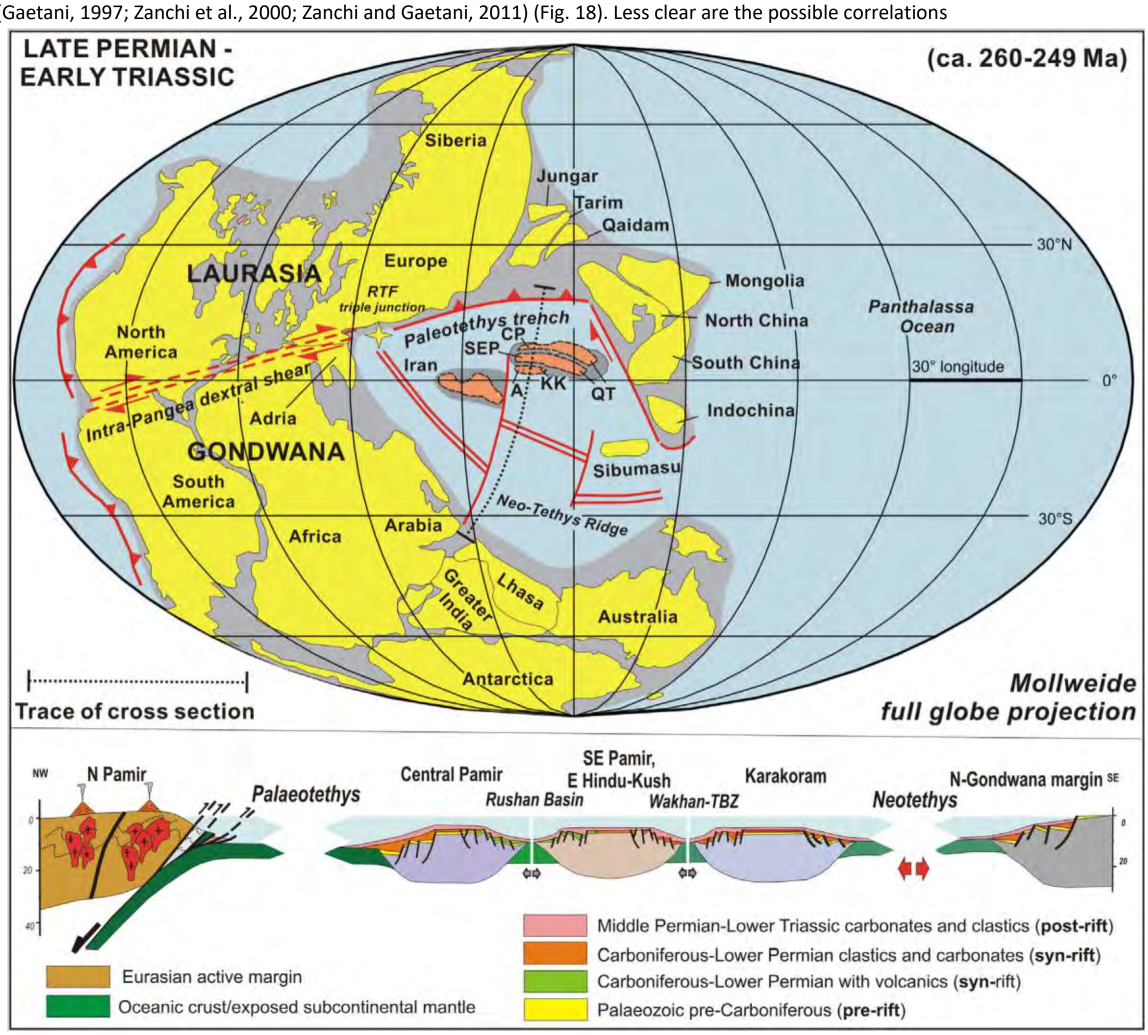

Fig. 18. Rifting and drifting of the Cimmerian blocks of Karakoram, SE Pamir and Central Pamir from the Eurasian margin. The belt was dissected by the oceanic basins of Rushan and Wakhan (modified from Muttoni et al., 2009; Angiolini et al., 2013a).

with extensional basins inside the laterally equivalent Qiangtang block (Schwab et al., 2004; Burtman, 2010; Robinson et al., 2012).

The Cimmerian terranes were subsequently involved in the Cimmerian orogeny with a progressively younger age of deformation from north to south. At the end of the Triassic, the accretion of Central Pamir to the Eurasian margin (N Pamir) produced the Jinsha suture (now marked by the Tanyimas Thrust zone) related to the closure of the Palaeotethys; more or less contemporaneously, the accretion of South Pamir to Central Pamir formed the Rushan-Pshart suture. Later, between the end of the Triassic and the Early Jurassic, the collision of Karakoram to South Pamir, with the formation of the TBZ (Angiolini et al., 2013a, Fig. 12), definitively accreted this block to Eurasia. In fact, the latter event is still not well constrained; Gaetani et al. (2013) leave open the age of the Ashtigar Formation, concluding that a Jurassic age cannot be excluded. The unconformable overlying Yashkuk Formation, interpreted as ''molassic red sandtones'' fed by the ''erosion of a foreland fold and thrust belt'' is Pliensbachian in age, so the collision remains bracketed between the latest Triassic and the Pliensbachian (Gaetani et al., 2013 p. 945).

Here, we document in detail the sedimentary evolution which records the first steps of this long term history, from the detachment of SE Pamir and Karakoram from Gondwana to the opening of the Rushan Ocean and finally to the involvement of the SE Pamir succession in the collision with Central Pamir.

Lateral variations in thickness and evidence of tectonic activity in the Pennsylvanian part of the Bazar Dara Group – as for instance the limestone boulders resedimented at the base of the Tashkazyk Formation (bed 3 of Grunt and Novikov, 1994) – suggest that this region was characterized by active extensional tectonics. The curves obtained from backstripping (Fig. 17) for this time interval are consistent with a rapid subsidence counterbalanced by terrigenous input and suggests that the Bazar Dara Group records the evolution of a rifted margin. Extensional tectonic activity is recorded also by the Pennsylvanian-Cisuralian successions of Karakoram (Gaetani et al., 1995, 2004) and was interpreted as the result of the Neotethys rifting south of Karakoram (Gaetani, 1997). In fact, these areas may provide just a farfield record of the opening of the Neotethys south of Karakoram and it is most probable that the formation of passive margins both along the northern side of the Karakoram terrane and in SE Pamir was related to the opening of small oceanic basins (respectively Wakhan and Rushan) inside the Cimmerian terranes (Fig. 18).

Tectonic subsidence accompanied by volcanic activity resumed in the late Early Permian (Kungurian) with the emission of the basalts of the Shindy Formation as shown in Fig. 13, the normalized trace elements concentrations of the Shindy basalts largely overlap with the reference Continental basalts pattern, particularly the fluid immobile elements such as Nb, Ta, Zr, Hf, Ti, HREE, and Sc. In this plot, the studied samples are also compared with the trace elements compositions of basalts from the Panjal Traps (white area in Fig. 9A-B; Vannay and Spring, 1993) and the Bhote Kosi lavas (blue area in Fig. 9B; Garzanti et al., 1999), interpreted as magmatic products of break-up and incipient sea-floor spreading in the Neotethys Ocean during the late Early Permian. The investigated samples from Mudzubulak and Kuristyk show a similar pattern to both the Lower Permian (mostly Artinskian-Kungurian) Himalayan basalts (Fig. 9B). A good similarity is evident from the comparison with Bhote Kosi, which show the same slight enrichment also in Th, Nb and P of the Shindy basalts with respect to the Panjal Traps. Concerning the LILE, our samples are more enriched, exception done for TZ17, which shows the same geochemical signature of samples from Bhote Kosi. Whether this enrichment in the Shindy basalts is due to a subsequent metamorphic chemical variation or to a crustal contamination during the magmatic activity is difficult to retrieve from the available data. In their work, Garzanti et al. (1999) indicate that the Lower Permian magmatism characterizing the newly formed northern margin of the Indian subcontinent is almost uniform from a geochemical point of view. The close affinity between lava flows in the Shindy Formation, the Panjal Traps and Bhote Kosi basalts, together with structural and sedimentary data may suggest that this volcanism occurred in an extensional setting. In particular, it may be related to the opening of the Rushan Ocean separating South and Central Pamir between the East and West Pshart blocks (Leven, 1995). In fact, the West Pshart zone is characterized by Lower Permian basalts, considered typical of continental rifting (Leven, 1995). Unfortunately, trace element compositions are not available for the volanics of the Phart zones.

Deepening of the basin, tectonic subsidence, active block faulting (indicated also by the synsedimentary record of conglomerates, breccias and huge olistoliths) and volcanic activity continued for most of the Middle Permian, but by the end of the Permian period the basin was filled by the volcaniclastic sandstones of the Takhtabulak Formation (Fig. 17A). The effects of the Middle Permian extensional or transtensional event are not recorded in the Kurteke platform (Fig. 17B). Here, volcaniclastics are only preserved at the base of the Kurteke Formation (upper Kungurian), and no increase in tectonic subsidence is evident for most of the Middle-Late Permian.

By the end of the Permian, SE Pamir consisted of basins and platforms comprised between the Rushan Ocean to the north and the Wakhan basin to the south (Fig. 18). The only available palaeomagnetic data, even if scanty and uncertain, are those provided by Davydov et al. (1982). Averaging their data (Davydov et al, 1982, tab. 1) and taking into account the number of samples (Dec = 43.8; Inc = 16.7, alpha (95%) = 11.2; R = 22.6376; k = 7.435; n = 6) the suggested palaeolatitude for the Takhtabulak Formation and Karatash Formation is 8.5 ± 7(Mattei, personal com.). So, by the Permian-Triassic boundary, the SE Pamir block should have been located slightly north of the equator (Fig. 18).

During the Early and Middle Triassic subsidence progressively increased and thick carbonate platforms could develop. As shown by the reversal trend in the curves of Fig. 17, from the Triassic onward, the subsidence of the SE Pamir basin was controlled by factors other than the opening of the Rushan basin, most probably the development of a subduction zone which leads to its closure at the end of the Triassic. Tectonic subsidence was very high during the deposition of the Upper Triassic flysches (Fig. 17), when SE Pamir was approaching Central Pamir. This was sharply followed by the closure of the basin taking to continental collision close to the Triassic–Jurassic boundary, as indicated by the spectacular angular unconformity at the base of the conglomerates of the Darbasatash Group, which record the erosion of a volcanic arc (Dronov et al., 2006 lexicon; Angiolini et al., 2013a).

To conclude, Karakoram and SE Pamir have a Palaeozoic Gondwanan ancestry and were subsequently involved in the Cimmerian orogeny; this is the oldest Mesozoic deformational event in the region, related to the formation of the Palaeotethys, Rushan-Pshart and TBZ sutures, producing respectively the accretion of Central Pamir to North Pamir and interposed arcs (Eurasian margin) and of South Pamir to Central Pamir at the end of the Triassic and finally of Karakoram to South Pamir slightly later.

13. Conclusions

The palaeontological, stratigraphical, sedimentological and geochemical data collected during three campaigns of fieldwork in the remote and logistically difficult to access regions of SE Pamir (Tajikistan) allowed a comprehensive reconstruction of the Permian-Triassic evolution of the area which provides further constrains on the differential motions of the Cimmerian terranes during the Permian. This accomplishes the understanding of the tectonic and stratigraphic evolution of the Late Palaeozoic sedimentary basins of the continental blocks accreted to Eurasia at the end of the Triassic.

Two main conclusions of broad significance can be drawn:

(1) Based on stratigraphic, sedimentological and geochemical data and subsidence analysis we have documented that SE Pamir had a Gondwanan ancestry, that it started to rift from Gondwana in the Pennsylvanian-Early Permian contestually with the formation of a passive margin facing the Rushan Ocean and possibly with the opening of the Wakhan basin separating the Pamirs from Karakoram. By the end of the Permian SE Pamir and related Cimmerian terranes should have lain slightly north of the equator. This was followed in the Triassic by the beginning of the closure of the ocean separating SE Pamir from Central Pamir and finally by the involvement of SE Pamir in the continental collision with Central Pamir and the Eurasian margin at the Triassic–Jurassic boundary (Cimmerian orogeny).
(2) The analyses of the fusulinids and conodonts of the Kubergandian and Murgabian stratotypes of SE Pamir provide the following correlation between the International (Global) and the Tethyan regional scales:
   – the upper Bolorian and the lower part of the Kubergandian correlate to the upper Kungurian;
   – the upper Kubergandian and the lower Murgabian correlate to the Roadian; the mid-upper Murgabian correlates to the Wordian;
   – possibly the uppermost Murgabian and the lower Midian correlate to the lower Capitanian.

So, the Kubergandian is now a well-characterized regional stage, based on fusulinids, ammonoids and conodonts and can be correlated to the Kungurian and the Roadian, whereas the Murgabian correlation – particularly the upper part – remains doubtful and should be investigated and resolved in Tethyan sections other than the SE Pamir ones, which have a poor fusulinid coverage.

Acknowledgements

LA, AZ, SZ and AN were supported by DARIUS PROGRAMME, Project CA11/01. V. Minaev, E. Kanaev, A. Niyazov and J. Mamadjanov are thanked for field assistance in the Pamirs and for permissions. CMH acknowledges Natural Sciences and Engineering Research Council for Discovery Grant funding. M. Stephenson, M. Santosh and an anonymous reviewer are warmly thanked for their thoughtful comments and revisions.
Appendix A. Supplementary material

Supplementary data associated with this article can be found, in the online version, at http://dx.doi.org/10.1016/j.jseaes.2014.
08.001.

References

Angiolini, L., Balini, M., Garzanti, E., Nicora, A., Tintori, A., Crasquin-Soleau, S., Muttoni, G., 2003. Permian climatic and palaeogeographic changes in northern Gondwana: the Khuff Formation of Interior Oman. Palaeogeogr. Palaeoclimatol. Palaeoecol. 191 (3–4), 269–300.
Angiolini, L., Gaetani, M., Muttoni, G., Stephenson, M.H., Zanchi, A., 2007. Tethyan oceanic currents and climate gradients 300 m.y. ago. Geology 35, 1071–1074.
Angiolini, L., Chaouachi, C., Soussi, M., Verna, V., Davydov, V.I., Henderson, C.M., Nicora, A., Rettori, R., Carabelli, L., 2008. New fossil findings and discovery of conodonts in the Guadalupian of Djebel Tebaga de Medenine: Biostratigraphic implications. Permophiles 51, Newsletter of the Subcommission on Permian Stratigraphy, pp. 10–21.
Angiolini, L., Baud, A., Changqun, C., Clapham, M.E., Davydov, V., Golubev, V., Grunt, T., Henderson, C.H., Jan, I.U., Kozur, H.W., Leven, E. Ya., Markov, A., Sa'ad Zeki AlMashaikie, Muttoni, G., Nicora, A., Rettori, R., Qinghua Shang, Shuzhong Shen, Stephenson, M.H., Katsumi Ueno, Wei Wang, Xiangdong Wang, Yue Wang, Yichun Zhang, 2010. Report of the Working Group: Neotethys, Paleotethys, and South China intraplatform basin correlations. Permophiles 54, Newsletter of the Subcommission on Permian Stratigraphy, pp. 14–26.
Angiolini, L., Zanchi, A., Zanchetta, S., Nicora, A., Vezzoli, G., 2013a. The Cimmerian geopuzzle: new data from South Pamir. Terra Nova 25, 352–360.
Angiolini, L., Crippa, G., Muttoni, G., Pignatti, J., 2013b. Guadalupian (Middle Permian) paleobiogeography of the Neotethys Ocean. Gondwana Res. 24, 173– 184.
Berra, F., Carminati, E., 2010. Subsidence history from backstripping analysis of the Permo-Mesozoic succession of the Central Southern Alps (Northern Italy). Basin Res. 22, 952–975.
Burtman, V.S., 2010. Tien Shan, Pamir, and Tibet: history and geodynamics of phanerozoic oceanic basins. Geotectonics 44 (5), 388–404.
Burtman, V.S., Molnar, P., 1993. Geological and geophysical evidence for deep subduction of continental crust Beneath the Pamir. Geol. Soc. Am. Spec. Pap. 281, 76.
Chediya, I.O., Davydov, V.I., 1980. About stratigraphic distribution of Colaniella (Foraminifera). Doklady Akademii Nauk USSR Report of Academy of Sciences of USSR, vol. 252 (4), 948–951 (in Russian).
Chediya, I.O., Bogoslovskaya, M.F., Davydov, V.I., Dmitriev, V.Yu., 1986. Fuzulinidy i ammonoidey v stratotipe kubergandinskogo yarusa (Yugo-Vostochnyy Pamir). Translated: Fusulinids and ammonoids in the stratotype of the Kubergandy Stage; southeastern Pamirs. Ezhegodnik Vsesoyuznogo Paleontologicheskogo Obshchestva 29, 28–53 (in Russian).
Chernykh, V.V., 2005. Zonal methods and biostratigraphy – zonal scale for Lower Permian of the Urals according to conodonts. Russian Academy of Sciences. Ekaterinburg, Russia, p. 217 (in Russian).
Chuvashov, B.I., Chernykh, V.V., Shen, S., Henderson, C.M., 2013. Proposal for the Global Stratotype Section and Point (GSSP) for the base-Artinskian Stage (Lower Permian). Permophiles 58, Newsletter of the Subcommission on Permian Stratigraphy, 26–34.
Colpaert, C., Monnet, C., Vachard, D., 2015. Middle Permian giant fusulinids of Afghanistan: morphometry of Eopolydiexodina and its implications for the central Tethyan paleogeography and the end-Guadalupian mass-extinction. J. Asian Earth Sci. 102, 127–145.
Crocket, J.H., Paul, D.K., 2004. Platinum-group elements in Deccan mafic rocks: a comparison of suites differentiated by Ir content. Chem. Geol. 208, 273–291.
Dagys, A.A., Dronov, V.I., 1989. First Conodonts from Triassic Sediments of the Southeastern Pamir. Doklady Akademii Nauk SSSR 309, 1469–1471 (in Russian).
Davydov, V.I., 1984. Murgabian Midian fusulinid Zonation and the problem of correlating the Murgabian/Midian Boundary on Global Scale. Abstracts and Programm Int. Symp. Perm. Stratigr. Environments & Resources. Guiyang, China, pp. 5–6.
Davydov, V.I., Komissarova, R.A., Khranov, A.N., Chediya, I.O., 1982. Paleomagnetism of upper Permian rocks of the Southeastern Pamirs. Doklady Akademii Nauk SSSR 267, 1177–1181.
Davydov, V.I., Krainer, K., Chernykh, V., 2013. Fusulinid biostratigraphy of the Lower Permian Zweikofel Formation (Rattendorf Group; Carnic Alps, Austria) and Lower Permian Tethyan chronostratigraphy. Geol. J. 48, 57–100.
Dmitriev, V.Y., 1976. Stratigraphy of the Lower Permian deposits of Southwestern Pamirs. Izvestiya Akademiya Nauk SSSR ser. Geol. vol. 6, pp. 81–87.
Domeier, M., Torsvik, T.H., 2014. Plate tectonics in the Late Paleozoic. Geosci. Front., doi: http://dx.doi.org/10.1016/j.gsf.2014.01.002.
Dronov, V.I., Leven, E.Y., 1960. The geology of the Southeastern Pamir. Sov. Geol. 11, 21–36 (in Russian).
Dronov, V.L., Leven, E.Y., 1990. Age of carbonate conglomerates of the central zone of SE Pamir. Doklady Akademi Nauk Tadjik SSR 25, 232–235 (in Russian).
Dronov, V.I., Luchnikov, V.S., 1976. Triassic System, in Subdivision of Stratified and Igneous Rocks of Tajikistan (Donish, Dushanbe), pp. 109–122 (in Russian).
Dronov, V.L., Melnikova, G.K., Salibajev, G.C., Bardashev, I.A., Minajiev, V.E., Muchabatov, M.M., 2006. Stratigraphic dictionary of the Pamir. Technische Universität Bergakademie Freiberg, pp. 252.
Dutkevich, G.A., 1937. Permian deposits of Central Asia. Probl. Sov. Geol. 7, 603–606 (in Russian).
Ebrahim-Nezhad E., Vachard, D., Asghar Siabeghodsy, A., Abbasi, S., 2014. MiddleLate Permian (Murgabian-Djulfian) foraminifers of the northern Maku area (western Azerbaijan, Iran). Palaeontologia Electronica (in press).
Gaetani, M., 1997. The Karakorum block in central Asia, from Ordovician to Cretaceous. Sed. Geol. 109, 339–359.
Gaetani, M., Leven, E.Y., 2014. The Permian succession of the Shaksgam Valley, Sinkiang (China). Ital. J. Geosci. 133, 45–62.
Gaetani, M., Garzanti, E., Jadoul, F., Nicora, A., Pasini, M., Tintori, A., Kanwar, S.A.K., 1990. The north Karakorum side of the Central Asia geopuzzle. Geol. Soc. Am. Bull. 102, 54–62.

Gaetani, M., Angiolini, L., Garzanti, E., Jadoul, F., Leven, E.Y., Nicora, A., Sciunnach, D., 1995. Permian stratigraphy in the Northern Karakorum, Pakistan. Riv. Ital. Paleontol. Stratigr. 101 (2), 112–158.

Gaetani, M., Zanchi, A., Angiolini, L., Olivini, G., Sciunnach, D., Brunton, H., Nicora, A., Mawson, R., 2004. The Carboniferous of the Western Karakorum (Pakistan). J. Asian Earth Sci. 23, 275–305.

Gaetani, M., Nicora, A., Henderson, C., Cirilli, S., Gale, L., Rettori, R., Vuolo, I., Adudorei, V., 2013. Refinements in the Upper Permian to Lower Jurassic stratigraphy of Karakorum, Pakistan. Facies 59, 915–948.

Garzanti, E., Le Fort, P., Sciunnach, D., 1999. First report of Lower Permian basalts in South Tibet: tholeiitic magmatism during break-up and incipient opening of Neotethys. J. Asian Earth Sci. 17, 533–546.

Garzanti, E., Vezzoli, G., Andò, S., Castiglioni, G., 2001. Petrology of rifted-margin sand (Red Sea and Gulf of Aden, Yemen). J. Geol. 109, 277–297.

Goldhammer, R.K., 1997. Compaction and decompaction algorithms for sedimentary carbonates. J. Sediment. Res. 67, 26–35.

Gorjunova, R.V., 1975. Permian Bryozoans from Pamirs. Moscow, Nauka (in Russian).

Grunt, T.A., Dmitriev, V.Y., 1973. Permian brachiopods of Pamirs. Trans. Paleontological Inst. 136, 1–211 (in Russian).

Grunt, T.A., Novikov, V.P., 1994. Biostratigraphy and biogeography of the early permian in the Southeastern Pamirs. Stratigr. Geol. Correl. 2 (4), 331– 339.

Henderson, C.M., 2014.The GSSP Process and the GSSPs proposed for baseSakmarian and base-Artinskian stages. Permophiles 59, Newsletter of the Subcommission on Permian Stratigraphy, pp. 13–17.

Henderson, C.M., Mei, S., 2003. Stratigraphic versus environmental significance of Permian serrated conodonts around the Cisuralian-Guadalupian boundary: new evidence from Oman. Palaeogeogr. Palaeoclimatol. Palaeoecol. 191, 301– 328.

Henderson, C.M., Mei, S., 2007. Geographical Clines in Permian and Lower Triassic Gondolellids and its role in taxonomy. Palaeoworld 16, 190–201.

Henderson, C.M., Davydov, V.I., Wardlaw, B.R., 2012. The Permian period. In: Gradstein, F., Ogg, J., Schmitz, M., Ogg, G. (Eds.), The Geologic Time Scale 2012, vol. 2. Elsevier, pp. 653–679 (Chapter 24).

Hofmann, A.W., 1988. Chemical differentiation of the Earth: the relationship between mantle, continental crust and oceanic crust. Earth Planet. Sci. Lett. 90, 297–314.

Hölzel, M., Faber, R., Wagreich, M., 2008. DeCompactionTool: software for subsidence analysis including statistical error quantification. Comput. Geosci. 34, 1454–1460.

Irvine, T.N., Baragar, W.R.A., 1971. A guide to the chemical classification of the common volcanic rocks. Can. J. Earth Sci. 8, 523–548.

Kobayashi, F., Ishii, K.I., 2003. Permian fusulinacean faunas of the Surmaq Formation in the Abadeh region, central Iran. Riv. Ital. Paleontol. Stratigr. 109 (2), 307–337.

Korchagin, O.A., 2008. Foraminifers and Stratigraphy of the Karatash Group (Lower Triassic–Middle Anisian), the Southeastern Pamir. Stratigr. Geol. Correl. 16 (3), 248–256.

Korchagin, O.A., 2009. Kaeveria fluegeli (Zaninetti, Altiner, Dager et Ducret, 1982) (Foraminifera) from Upper Triassic of the South-East Pamirs. Stratigr. Geol. Correl. 17 (1), 62–67.

Kozur, H., 1994. Permian pelagic and shallow-water conodont zonation. Permophiles 24, Newsletter of the Subcommission on Permian Stratigraphy, 16–20.

Kozur, H., Wardlaw, B.R., 2010. The Guadalupian conodont fauna of Rustaq and Wadi Wasit, Oman and a West Texas connection. Micropaleontology 56, 213– 231.

Kushlin, B.K. 1973. Pamir Geosyncline. Stratigraphy of the USSR. Triassic System (Nedra, Moscow), pp. 374–394 (in Russian).

Leonova, T.B., Dmitriev, V.Y., 1989. Early Permian ammonoids in SE Pamirs. Transactions of Paleontological Institute, vol. 235, pp. 1–298, Moscow (in Russian).

Leven, E.Y., 1958. Permian deposits of SE Pamirs. Abstracts of the meeting in unification of stratigraphic correlation chart in Central Asia. Tashkent, pp. 95– 100 (in Russian).

Leven, E.Y., 1963. O filogenii vysskikh fuzulinid i raschlenenii verkhnepermskikh otlozhenii Tetisa (On the phylogeny of advanced fusulinids and subdivision of Tethyan Late Permian deposits). Vopr. Mikropaleontol. 7, 57–70 (in Russian).

Leven, E.Y., 1967. Stratigraphy and fusulinids of Permian deposits of Pamirs. Transaction of Geological Institute of Academy of Science of U.S.S.R. 167, pp. 224 (in Russian).

Leven, E.Y., 1979. Bolorian Stage of the Permian: Substantiation, Characteristics, Correlation. Izvestiya Akademiya Nauk SSSR Ser. Geol., vol. 1, pp. 53–65.

Leven, E.Y., 1980. Explanatory notes for the Stratigraphic Scale of Permian deposits of the Tethyan Region. Transactions of VSEGEI, 3–51, Leningrad (in Russian).

Leven, E.Y., 1981. Permian Tethys Stage Scale and correlation of sections of the Mediterranean-Alpine folded belt. In: Karamata, S., Sassi, F.P. (Eds.), IGCP No. 5. Newsletter 3, pp. 100–112.

Leven, E.Y., 1992. Problems of Tethyan Permian stratigraphy. Int. Geol. Rev. 34 (10), 976–985.

Leven, E.Y., 1995. Permian and Triassic of the Rushan-Pshart Zone (Pamir). Riv. Ital. Paleontol. Stratigr. 101, 3–16.

Leven, E.Y., 1998. Permian fusulinids assemblages of the Transcaucasia. Riv. Ital. Paleontol. Stratigr. 104, 299–328.

Leven, E.Y., 2001. On possibility of using the global permian stage scale in the Tethyan region. Stratigr. Geol. Correl. 9 (6), 118–131.

Leven, E.Y., Bogoslovskaya, M.F., 2006. The Roadian stage of the permian and problems of its global correlation. Stratigr. Geol. Correl. 14 (2), 164–173.

Leven, E.Y., Shcherbovich, S.F., 1978. Fusulinids and Stratigraphy of the Asselian Stage in Darvaz (Nauka, Moscow, 1978), pp. 162, (in Russian).

Leven, E.Y., Shcherbovich, S.F., 1980. Fusulinid assemblages of the Darvaz Sakmarian Stage. Voprosy Micropaleontologii 23, 71–85 (in Russian).

Leven, E.Y., Grunt, T.A., Dmitriev, V.Y., 1983. Bolorian stage of the Permian: Type Sections. Izvestiya Akademiya Nauk SSSR Ser. Geol., vol. 8, pp. 35–45 (in Russian).

Leven, E. Y., Dmitriev, V.Y., Novikov, V.P., 1989. Explanatory note to the regional stratigraphic scheme of Permian deposits of Central Asia (Pamir subregion). Publisher ''Donish'', Dushanbe, pp. 1–60 (in Russian).

Leven, E.Y., Leonova, T.B., Dmitriev, V.Y., 1992. Permian of the Darvaz-Transalay Zone of Pamirs: Fusulinids, Ammonoids, Stratigraphy. Trudy Paleontol. Inst. RAN 253, pp. 1–197 (in Russian).

Lightfoot, P.C., Hawkesworth, C.J., Devey, C.W., Rogers, N.W., Van Calsteren, P., 1990. Source and differentiation of Deccan trap lavas: implications of geochemical and mineral variations. J. Petrol. 31, 1165–1200.

Lucas, S., 2014. Two Recently Proposed Lower Permian GSSPs. Permophiles 59, Newsletter of the Subcommission on Permian Stratigraphy, pp. 6–7.

McDonough, W.F., 1994. Chemical and isotopic systematics of continental lithospheric mantle. In: Meyer, H.O.A., Leonardos, O.H. (Eds.), Kimberlites, Related Rocks and Mantle Xenoliths, vol. 1 C.P.R.M., Brasilia, pp. 478–485.

McDonough, W.F., Sun, S.S., 1995. Composition of the earth. Chem. Geol. 120, 223– 253.

Mei, S., Henderson, C.M., 2001. Evolution of Permian conodont provincialism and its significance in global correlation and paleoclimatic implication. Palaeogeogr. Palaeoclimatol. Palaeoecol. 170, 237–260.

Mei, S., Henderson, C.M., 2002. Conodont definition of the Kungurian (Cisuralian) and Roadian (Guadalupian) Boundary. In: Hills, L.V., Henderson, C.M., Bamber, E.W. (Eds.), Carboniferous and Permian of the World. Canadian Society of Petroleum Geologists, Memoir, vol. 19, pp. 529–551.

Mei, S., Henderson, C.M., Wardlaw, B.R., 2002. Evolution and distribution of the conodonts Sweetognathus and Iranognathus and related genera during the Permian and their implications for climate change. Palaeogeogr. Palaeoclimatol. Palaeoecol. 180, 57–91.

Meschede, M., 1986. A method of discriminating between different types of midocean ridge basalts and continental tholeiites with the Nb-Zr-Y diagram. Chem. Geol. 56, 207–218.

Miklukho-Maklay, A.D., 1958. On Stage subdivision on marine Permian deposits of the USSR southern regions. Doklady Akademii Nauk SSSR 120, pp. 175–178.

Muttoni, G., Gaetani, M., Kent, D.V., Sciunnach, D., Angiolini, L., Berra, F., Garzanti, M., Mattei, M., Zanchi, A., 2009. Opening of the Neo-Tethys Ocean and the Pangea B to Pangea A transformation during the Permian. GeoArabia 14, 17–48.

Ning, Z., Henderson, C.M., Wenchen, X., 2010. Conodonts and radiolarian through the Cisuralian-Guadalupian boundary from the Pingxiang and Dachongling sections, Guangxi region, South China. Alcheringa 34 (2), 135–160.

Novikov, V.P., 1976. Stratigraphy of Bazardara series in North Alichur Ridge (SE Pamirs). Report of Academy of Sciences of Tadzhik SSR, vol. 19, no. 3, pp. 38–41 (in Russian).

Novikov, V.P., 1979. Main section types of the Bazardara Group in Southeastern Pamirs. Izvestiya Akademiya Nauk SSSR Ser. Geol. vol. 7, pp. 61–70.

Orchard, M.J., 2007. Conodont diversity and evolution through the latest Permian and Early Triassic upheavals. Palaeogeogr. Palaeoclimatol. Palaeoecol. 252, 93– 117.

Pashkov, B.R., Budanov, V.I., 1990. Tectonics of the SW–SE Pamir junction. Geotectonics 24, 246–253.

Pavlov, A.M., 1972. Stratigraphy and ammonoids of Upper Paleozoic in SE Pamirs. Abstract of PhD dissertation, Leningrad, pp. 21 (in Russian).

Pearce, J.A., Norry, M.J., 1979. Petrogenetic implications of Ti, Zr, Y, and Nb variations in volcanic rocks. Contrib. Miner. Petrol. 69, 33–47.

Peng, Z.X., Mahoney, J.J., Hooper, P.R., Macdougall, J.D., Krishnamurthy, P., 1998. Basalts of the northeastern Deccan Traps, India: isotopic and elemental geochemistry and relation to southwestern Deccan stratigraphy. J. Geophys. Res. 103, 29843–29865.

Reimers, A.N., 1991. Permisky conodonti Pamir i Darvazi. Bjul MOIP Odtel. Geol. 66 (5), 59–71 (in Russian).

Reimers, A.N., 1999. Conodonts of the Lower Permian in the Urals, Caspian Region, and Pamirs. GEOS, pp. 211, Moscow (in Russian).

Replumaz, A., Capitanio, F.A., Guillot, S., Negredo, A.M., Villaseñor, A., 2014. The coupling of Indian subduction and Asian continental tectonics. Gondwana Res.

26, 608–626.

Ritter, S.M., 1987. Biofacies-based refinement of Early Permian conodont biostratigraphy, in central and western USA. In: Austin, R.A. (Ed.), Conodonts – Investigative Techniques and Applications. British Micropalaeontological Society Series. Ellis Horwood Ltd., Chichester, England, pp. 382–403.

Robinson, A.C., Ducea, M., Lapen, T.J., 2012. Detrital zircon and isotopic constraints on the crustal architecture and tectonic evolution of the northeastern Pamir. Tectonics 31. http://dx.doi.org/10.1029/2011TC003013.

Ruzhentsev, V.E., 1954. Asselian stage of the Permian System. Doklady Akademii Nauk SSSR 99 (6), 1079–1082 (in Russian).

Ruzhentsev, V.E., 1978. Asselian Ammonoids from Pamirs. Paleontological J. 1, 36–52.

Ruzhentsev, V.E., Shvol'man V.A., 1981. Tectonics and structure of the Pamir metamorphics. In: Saklani P.S. (Ed.), Metamorphic Tectonites of the Himalaya, pp. 27–41.

Scheck, M., Bayer, U., 1999. Evolution of the Northeast German Basin – inferences from a 3D structural model and subsidence analysis. Tectonophysics 313, 145– 169.

Schmidt, J., Hacker, B.R., Ratschbacher, L., Stübner, K., Stearns, M., Kylander-Clark, A., Cottle, J.M., Alexander, A., Webb, G., Gehrels, G., Minaev, V., 2011. Cenozoic deep crust in the Pamir. Earth Planet. Sci. Lett. 312, 411–421.

Schmoker, J.W., Halley, R.B., 1982. Carbonate porosity versus depth: a predictable relation for south Florida. Am. Assoc. Pet. Geol. Bull. 66, 2561–2570.

Schwab, M., Ratschbacher, L., Siebel, W., McWilliams, M., Minaev, V., Lutkov, V., Chen, F., Stanek, K., Nelson, B., Frisch, W., Wooden, J.L., 2004. Assembly of the Pamirs: age and origin of magmatic belts from the southern Tien Shan to the southern Pamirs and their relation to Tibet. Tectonics 23, TC4002, doi: http:// dx.doi.org/10.1029/2003TC001583.

Sclater, J.G., Christie, P.A.F., 1980. Continental stretching: an explanation of the post-Mid-Cretaceous subsidence of the Central North Sea Basin. J. Geophys. Res. 85 (B7), 3711–3739.

Sengör, A.M.C., 1979. Mid-Mesozoic closure of Permo-Triassic Tethys and its implications. Nature 279, 590–593.

Shen, S.Z., Yuan, D.Z., Henderson, C.M., Tazawa, J., Zhang, Y.C., 2013. Implications of Kungurian (Early Permian) conodonts from Hatahoko, Japan, for correlation between the Tethyan and international timescales. Micropaleontology 58 (6), 505–522.

Sleep, N.H., 1971. Thermal effects of the formation of Atlantic continental margin by continental breakup. Geophys. J. Roy. Astron. Soc. 24, 325–350.

Stübner, K., Ratschbacher, Rutte, D., Sperner, Stanek, K., Minaev, V., Wiesinger, M., Gloaguen, R., Project TIPAGE members, 2013a. The giant Shakhdara migmatitic gneiss dome, Pamir, India-Asia collision zone: 1. Geometry and kinematics. Tectonics 32, 948–979.

Stübner, K., Ratschbacher, L., Weise, C., Chow, J., Hofmann, J., Khan, J., Rutte, D., Sperner, B., Pfänder, J.A., Hacker, B.R., Dunkl, I., Tichomirowa, M., Stearns, M.A., Project TIPAGE members, 2013b. The giant Shakhdara migmatitic gneiss dome, Pamir, India-Asia collision zone: 2. Timing of dome formation. Tectonics, vol. 32, pp. 1404–1431.

Suarez Riglos, M., Hunicken, M.A., Merino, D., 1987. Conodont biostratigraphy of the Upper Carboniferous-Lower Permian rocks of Bolivia. In: Austin, R.A., (Ed.), Conodonts – Investigative Techniques and Applications. British Micropalaeontological Society Series, Ellis Horwood Ltd., Chichester, England, pp. 316–332.

Sun, S.S., McDonough, W.F., 1989. Magmatism in Ocean Basins Chemical and Isotopic Systematics of Ocean Basalts: Implications for Mantle Composition and Processes. Geological Society of London, London, vol. 42, pp. 313–345.

Vachard, D., 1980. Téthys et Gondwana au Paléozoïque supérieur – Les données afghanes-biostratigraphie, micropaléontologie, paléogéographie. Documents et Travaux IGAL, Paris (2 volumes) 2, pp. 1–463.

Vachard, D., Montenat, C., 1996. The Carboniferous of Afghanistan. In: Wagner, R. (Ed.), Carboniferous of the World, vol. 3, pp. 459–487.

Van Hinte, J.E., 1978. Geohistory analysis – application of micropaleontology to exploration geology. Am. Assoc. Pet. Geol. Bull. 62, 201–222.

Vannay J.C., Spring L., 1993. Geochemistry of the continental basalts within the Tethyan Himalaya of Lahul-Spiti and SE Zanskar, northwest India. Geological Society, London, Special Publications, vol. 74, pp. 237–249.

Vlasov, N.G., Dyakov, Y.A., Cherev, E.S., 1991. Geological map of the Tajik SSR and adjacent territories, 1:500,000. VSEGEI (Vsesojuznoi Geol. Inst.) Leningrad, Saint Petersburg.

Yin, A., Harrison, T.M., 2000. Geologic evolution of the Himalayan-Tibetan Orogen. Annu. Rev. Earth Planet. Sci. 28, 211–280.

Zanchetta, S., Berra, F., Zanchi, A., Bergomi, M., Caridroit, M., Nicora, M., Heidarzadeh, G., 2013. The record of the Late Palaeozoic active margin of the Palaeotethys in NE Iran: constraints on the Cimmerian orogeny. Gondwana Res. 24, 1237–1266.

Zanchi, A., Gaetani, M., 2011. The geology of the Karakoram range, Pakistan: the new 1:100,000 geological map of Central-Western Karakoram. Ital. J. Geosci. 130, 161–262.

Zanchi, A., Poli, S., Fumagalli, P., Gaetani, M., 2000. Mantle exhumation along the Tirich Mir Fault Zone, NW Pakistan: pre mid-Cretaceous accretion of the Karakoram terrane to the Asian margin. In: Khan, M.A., Treloar, P.J., Searle, M.P., Jan, M.Q. (Eds.), Tectonics of the Nanga Parbat Syntaxis and the Western Himalayas. Geological Society of London Special Publication, vol. 170, pp. 237– 252.

Zanchi, A., Zanchetta S., Berra, F., Mattei, M., Garzanti, E., Molyneux, S., Nawab, A., Sabouri, J., 2009. The Eo-Cimmerian (Late? Triassic) orogeny in north Iran. In: Brunet, M.F., Wilmsen, M., Granath, J.W., (Eds.), South Caspian to Central Iran Basins. Geological Society of London Special Publications, vol. 312, pp. 31–55.